NanoSpire

Photo: L. A. Crum

DISCOVERY OF MACROCATIONIC CRYSTALLINE H2O CAVITATION REENTRANT JETS & THEIR ROLE IN CAVITATION ZERO POINT ENERGY, FUSION & THE ORIGIN OF LIFE

The Seventh Annual Conference on the Physics, Chemistry & Biology of Water, October 18-21, 2012

Presentation Co-Sponsored by Vermont Photonics and the Maine Space Grant Consortium
MSGC Director's Fund Grant SG-13-22

Mark L. LeClair, CEO NanoSpire, Inc.
P.O. Box 734 Gorham, ME 04038
mleclair@nanospireinc.com
207.929.6226

Abstract. Macrocationic, crystallized cavitation reentrant jets were first observed during investigation of directed cavitation reentrant jet nano and micro-machining in water by the author in 2004 in Buxton, ME, on grants funded by the Maine Technology Institute. I again observed the same behavior in 2005 on work funded by the New York State Energy Research and Development Authority as PI, with co-investigators Serge Lebid, EVP NanoSpire, Inc., Prof. Eric Eisenbraun of Albany Nanotech, and others. The extreme pressure and temperature of cavitation bubble collapse was compressing dissociated water H+ and OH- ions at the bubble interface into solid, faceted macrocationic crystals possessing an equilateral triangle crystalline subunit. Reentrant jet impacts formed pit cross-sections that were equilateral triangles, regular or oval-shaped hexagons, twinned crystals such as hourglasses, or hybrids of triangles and hexagons. The presentation will provide an overview of data and theories addressing the structure and dynamics of crystallized cavitation reentrant jets in coherently extracting zero point energy, triggering fusion and driving prebiotic chemistry.

The cavitation reentrant jet crystal has enormous positive electrostatic charge concentration and induces a negative charge on the surface of any nearby object. Electrostatic attraction then draws the positive crystal towards its negative induced charge on a nearby surface and imbeds the crystal with great force, imprinting a fossil image of the crystal's facets in a wide variety of materials. The crystalline structure presents a concentrated number of protons on the surface giving it a very low pH. Bright red hexagon jet impact pits in green litmus and purple hexagon pits in orange litmus all indicated zero pH. The crystal is short-lived, typically persisting for a few microseconds in water, isolated by a super-cavitating water vapor column. The crystals can form linear or helical strands, with large bacteriophage-like icosahedral hexagonal heads and long narrow whip tails and can join head to toe, forming coils that can also supercoil, like DNA. A new diamond-like tetrahedral SP3 orbital structure is proposed, based on the crystal's subunit equilateral triangular structure and dissociated water composition. The proposed molecular structure makes the crystal twice as strong as a diamond and up to 5.5 times denser than ordinary water. Sinusoidal reentrant jet buckling data used with the Euler equation indicates that the crystal is ten times stiffer than tungsten.

The cavitation reentrant jet water crystal plays a central role in coherently extracting zero point energy via the LeClair Effect, which triggered intense fusion, fission and transmutation in water during grant funded landmark experiments conducted August 24-25, 2009 in Buxton, ME by Mark L. LeClair and Serge Lebid of NanoSpire, Inc., that produced 2900 watts of hot water flow from 840 watts of electrical input. The transmuted material has been analyzed by SEM-EDAX, XPS and LA-ICP-MS, revealing that the transmuted material was generated by small scale supernova nucleosynthesis forming on the supersonic bow shock surrounding the crystal. Seventy-eight elements were detected, along with short-lived isotopes.

Crystallized cavitation reentrant jets are also the template for the origin of life. Observed large scale cavitation nucleosynthesis seriously challenges the paradigm that supernovas were the primary providers of the building blocks of life. I presented my theory to the NASA Astrobiology Institute in 2001 that cavitation reentrant jets generated by the underwater wake of asteroid and comet ejecta impacting into oceans and lakes during the primordial bombardment generated life. Cavitation was also generated from volcanic eruptions, lightning strikes, wave action and other natural phenomena. Helical cavitation reentrant jets act are exact geometric and molecular templates for the assembly of DNA, RNA and protein. The correct size protein, RNA and DNA reentrant jet templates only form within the same submicron size range where cavitation induces and accelerates unusual chemical reactions. The crystals can join head to toe, just as RNA and DNA 3’ and 5’ ends do, forming helical coils that can be relaxed, or twist and writhe into supercoils. The discovery of the crystal and its effects will have a dramatic impact on the physics, chemistry and biology of water.

About NanoSpire

NanoSpire's business focus and expertise is harnessing cavitation at a fundamental level. NanoSpire, Inc. is a privately held IP holding corporation. We are currently pursuing licensing, JV and product development in many areas with key strategic partners

- Incorporated January, 2002
- Winner of Seven Grants (NY-NYSERDA, ME-MTI, MSGC, Hub Labs)
- Winner of Innovation Technology Award, Nano Tech 2003 + Future Conference, Tokyo, Japan
- Issued Four Fundamental Patents in 2005-2009 for Creating & Controlling High-Speed Cavitation Reentrant Jets Useful in a Broad Array of Applications

NanoSpire Team

Mark L. LeClair, Founder, President & CEO: *30 yrs expertise in cavitation. Proprietor of CFD Associates. Former Trident II underwater launch hydrodynamicist, Lockheed Missiles & Space Co. Worcester Polytechnic Institute (WPI) graduate in mechanical engineering (MSME, BSME w/distinction) with concentration in fluid dynamics, heat transfer, thermodynamics, physics and nuclear engineering*

Serge Lebid, *EVP & Cofounder: Former VP and founder of Five Star Technologies, Inc., a cavitation-based nanophase materials company.*

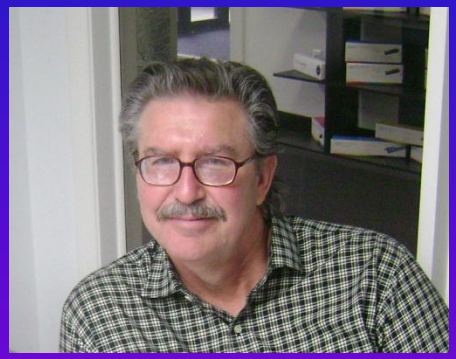

Cavitation Reentrant Jet Patents

Five Key platform US patents granted:

LeClair, M. L., *Method and Apparatus for the Controlled Formation of Cavitation Bubbles*. US Patent No. 7,517,430 issued Apr. 14, 2009

LeClair, M. L., *Method and Apparatus for the Controlled Formation of Cavitation Bubbles,* US Patent 7,297,288, Issued Nov. 20, 2007

LeClair, M. L., *Method and Apparatus for the Controlled Formation of Cavitation Bubbles,* US Patent 6,960,307, Issued Nov. 1, 2005

LeClair, M. L., *Method and Apparatus for the Controlled Formation of Cavitation Bubbles Using Target Bubbles,* US Patent 6,932,914, Issued Aug. 23, 2005

LeClair, M. L , et. al., *Method and Apparatus for Producing Liquid Suspensions of Finely Divided Matter*, U.S. Patent No. 5,522,553 a high-shear cavitating rotor-stator mixing device. Issued June 4, 1996.

What is Cavitation?

- Cavitation bubbles are created when an object passes through a liquid rapidly or when a liquid is brought to its boiling point
- Cavitation bubbles collapse asymmetrically next to an object, causing a high speed liquid jet to shoot towards the object
- The cavitation "reentrant jet" exits the bubble at up to Mach 4 and can drill a hole through a diamond
- This behavior is very repeatable. The size, force and direction of the reentrant jet can be controlled and produced with precision using a laser, ultrasound, x-rays, etc.

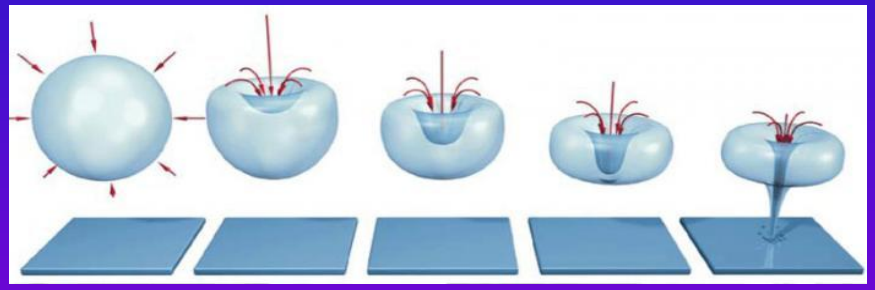

Cavitation Collapse Sequence

US Patents 7,517,430& 6,960,307, *Method and Apparatus for the Controlled Formation of Cavitation Bubbles, M. L. LeClair*

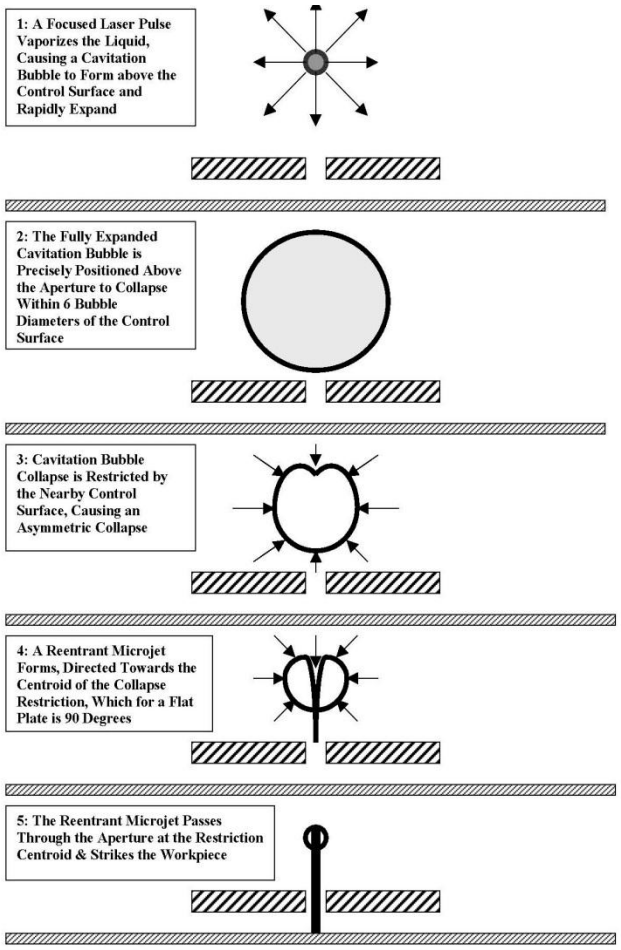

US Patents 7,297,288 & 6,932,914, *Method and Apparatus for the Controlled Formation of Cavitation Bubbles Using Target Bubbles, M. L. LeClair*

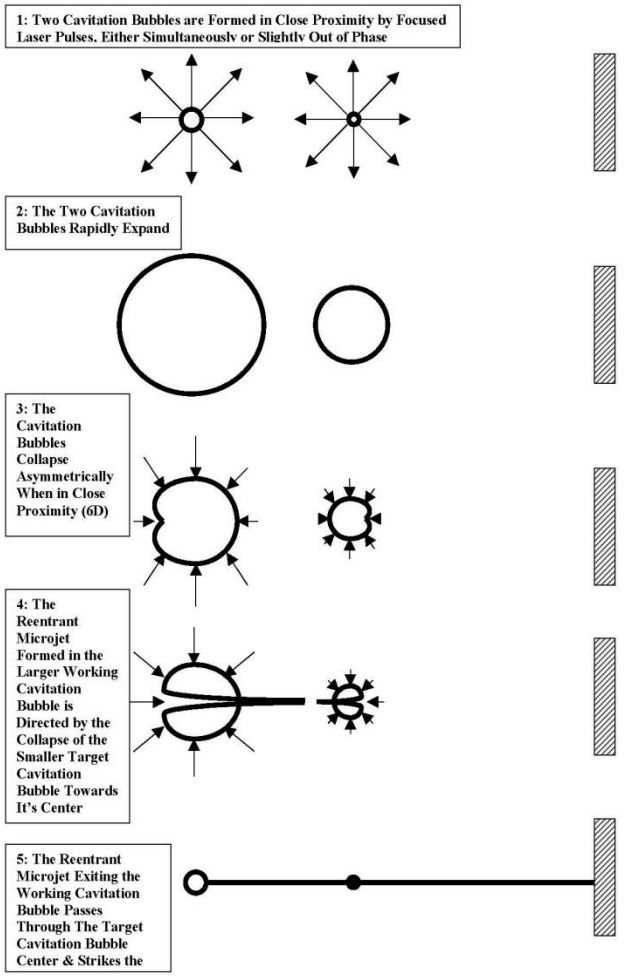

NanoSpire Product Schematics

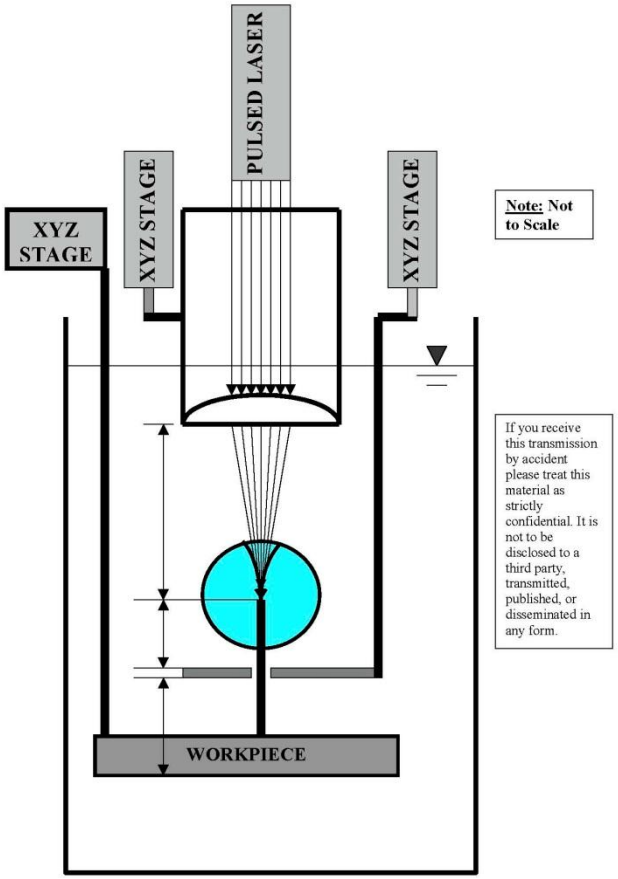

US Patents 7,517,430& 6,960,307, *Method and Apparatus for the Controlled Formation of Cavitation Bubbles, M. L. LeClair*

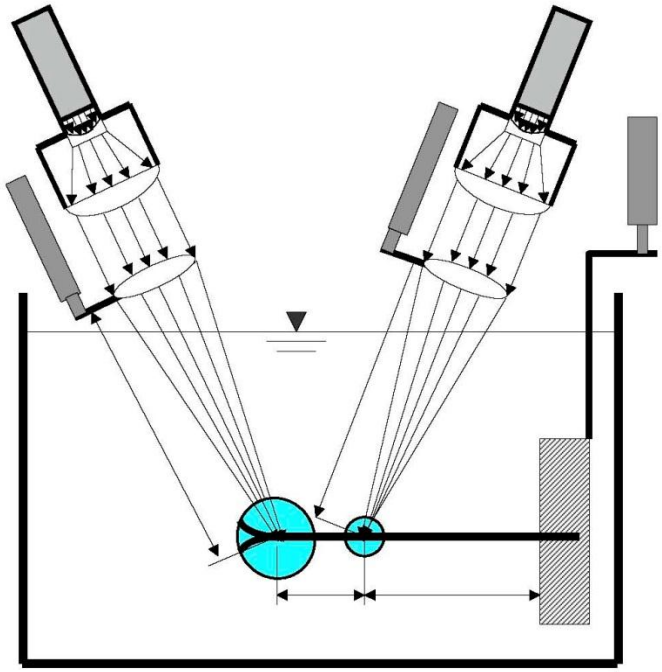

US Patents 7,297,288 & 6,932,914, *Method and Apparatus for the Controlled Formation of Cavitation Bubbles Using Target Bubbles, M. L. LeClair*

Cavitation Reentrant Jet Micro/Nanofabrication Technology

- Top Down: Drill, cut, mill, anneal, shotpeen, materials at a few nanometers
- Bottom Up: Weld, coat, implant, & assemble nanostructures
- Process Wide range of materials (diamond, glass, silicon, ceramics, metals, etc.)
- Up to 500 kHz cutting potential

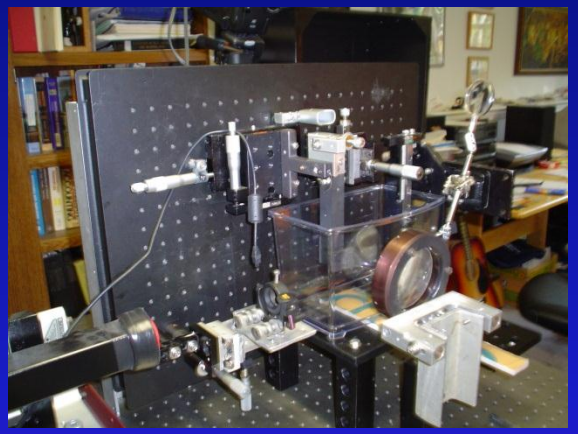

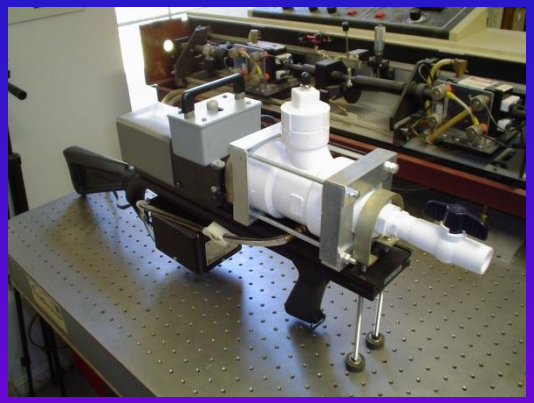

- Nanophase & Engineered Materials
- Coatings
- Sensors
- MEMS/NEMS
- Micro/Nano Fabrication
- Biotechnology
- Solar Energy
- Cavitation Powered Drill Bits for Oil & Gas Exploration
- Breakthrough Biodiesel Production

NanoSpire, Inc.

Micro-Hole Drilling Registration Accuracy

First Results Funded by Maine Technology Institute Achieved a +/- 1.27 Degree Average Accuracy with a Repeatability of 0.25 Degrees Standard Deviation

SEM Photos Courtesy of Albany Nanotech, MTI SG1424

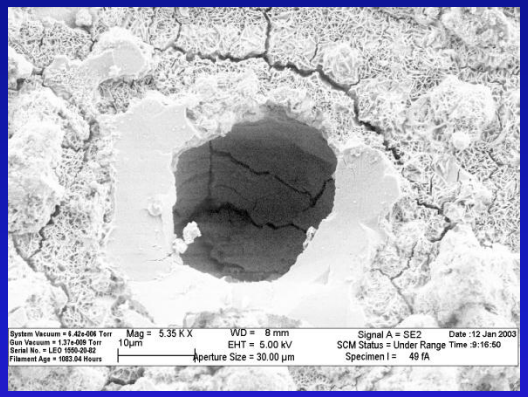

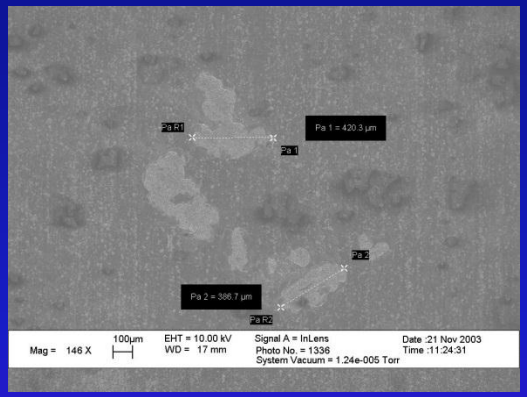

Machining of Linear Array in Glass
100X Mag
Pit size: 30 Microns,
Spacing: 300 Microns
MTI Grant SG1424

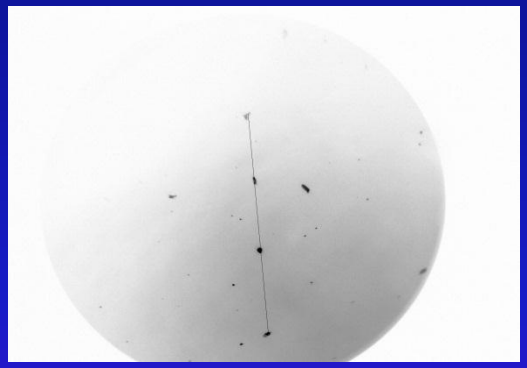

Later Results Improved to +/- 0.08 Degrees Accuracy, Grant Funded by New York State Energy Research & Development Authority, Grant Agreement #8250

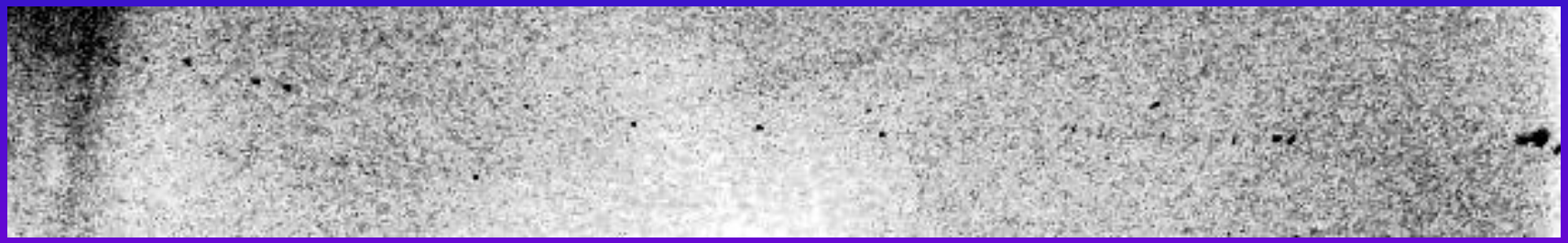

NanoSpire Nanomaterials Processes

- Dispersion
- Emulsification
- Cell Rupture
- Homogenization
- High Shear Mixing
- Microencapsulation
- Wet Milling
- Nanomaterials Synthesis

NanoSpire Nanomaterials Markets

- Biotech
- Cosmetics
- Chemicals
- Dairy
- Food/Beverage
- Ceramics
- Engineered materials
- Semiconductors
- Catalysts
- Inks/Paints/Coatings
- Polymers
- Personal Care
- Petrochemical
- Composites
- Ceramics
- Nanotubes / Nanowires
- Waste & Water Treatment

Cavitation Reentrant Jet High-Shear Mixers

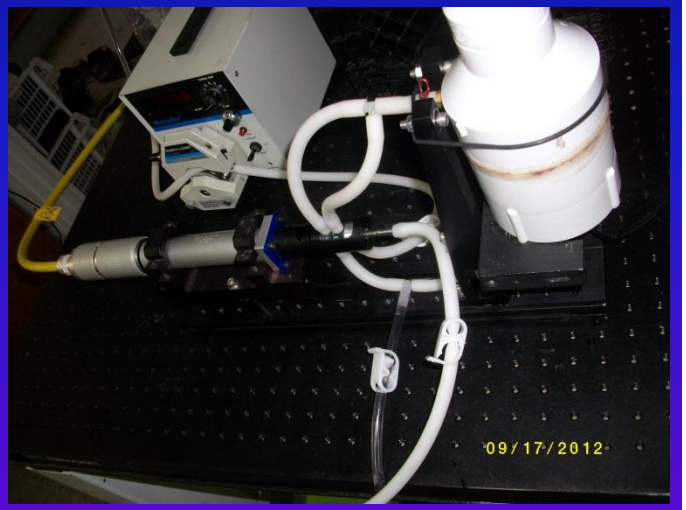

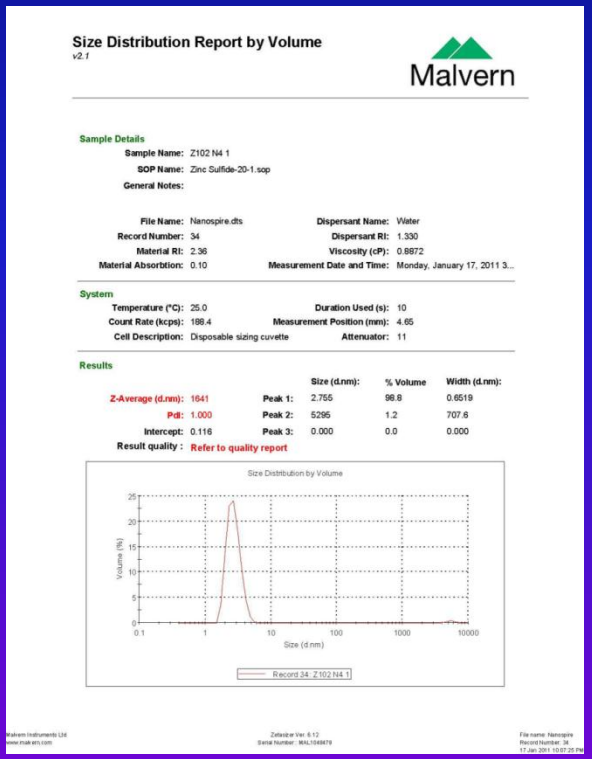
Size Distribution Report by Volume
v2.1

Malvern

Sample Details
Sample Name: Z102 N4 1
SOP Name: Zinc Sulfide-20-1.sop
General Notes:

File Name: Nanospire.dts
Record Number: 34
Material RI: 2.36
Material Absorbtion: 0.10
Dispersant Name: Water
Dispersant RI: 1.330
Viscosity (cP): 0.8872
Measurement Date and Time: Monday, January 17, 2011 3...

System
Temperature (°C): 25.0
Count Rate (kcps): 188.4
Cell Description: Disposable sizing cuvette
Duration Used (s): 10
Measurement Position (mm): 4.65
Attenuator: 11

Results

		Size (d.nm):	% Volume	Width (d.nm):
Z-Average (d.nm): 1641	Peak 1:	2.755	98.8	0.6519
PdI: 1.000	Peak 2:	5295	1.2	707.6
Intercept: 0.116	Peak 3:	0.000	0.0	0.000

Result quality : Refer to quality report

Size Distribution by Volume
Volume (%)
Size (d.nm)
Record 34: Z102 N4 1

10/20/2012

NanoSpire, Inc.

NanoSpire Grants

Discovery Of Macrocationic Crystalline H2O Cavitation Reentrant Jets & Their Role In Cavitation Zero Point Energy, Fusion & The Origin Of Life, Mark L. LeClair. An invited presentation given at the Mt Snpw Resort, W. Dover, VT. Travel funded by the Water 2012 Conference Organizers & Maine Space Grant Consortium (MSGC) Directors Fund Grant SG-13-22.

Utilization of Crystallized Cavitation Reentrant Jets for Zero Point Energy Production Principal Investigator: Mark L. LeClair, CEO, NanoSpire, Inc., Coinvestigator: Serge Lebid, Exec. VP, NanoSpire, Inc. Final Report to HUB LAB Limited, a BVI Limited Company. Oct. 12, 2009.

Turbo Pump Cavitation Tools, Proposal submitted to Air Force SBIR, Maine Technology Institute (MTI) Phase Zero PZ059 for grant writing support. Feb. 7, 2008.

Feasibility Study for Cavitation Nanofabrication Technology for Oxygen Sensor Manufacturing , New York State Energy Research and Development Authority (NYSERDA), Agreement #8250. Principal Investigator, NanoSpire, Inc.: Mark L. LeClair (Pres. & CEO), Serge Lebid, (Exec VP), Sencer, Inc.: David Burt (Pres.), Jason Voellinger (Eng.). Consultants: Albany NanoTech, Deloitte & Touche, Cientifica. Final Report submitted Feb. 28, 2006.

Cavitation Machining Product Development, Maine Technology Institute (MTI) Seed Grant SG1803. Principal Investigator: Mark L. LeClair. Final Report to the Maine Technology Institute, Nov. 18, 2004.

Cavitation Machining Prototype Development, Maine Technology Institute (MTI) Seed Grant SG1424. Principal Investigator: Mark L. LeClair. Final Report to the Maine Technology Institute, Feb. 28, 2004.

Business Plan Development for Cavitation Nano-CNC, Maine Technology Institute (MTI) Seed Grant SG740. Principal Investigator: Mark L. LeClair, Co-Investigators: Todd Dunn & Susan LeClair. Final Report to the Maine Technology Institute, April 24, 2002.

Cavitation and Origins of Life, by Mark L. LeClair, Principal, CFD Associates. An invited seminar presented to NASA Ames Research Center, Mt. View, CA. Seminar sponsored by the Maine Space Grant Consortium Director's Discretionary Fund. Presented July 30, 2001.

Cavitation Erosion and Fusion

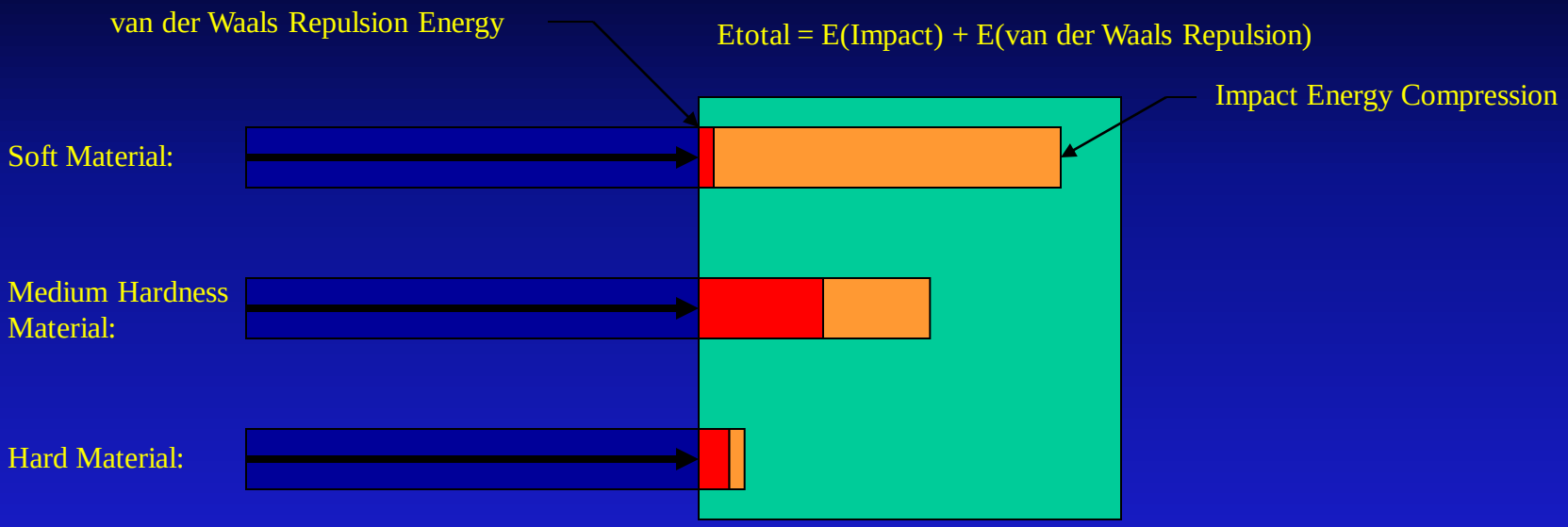

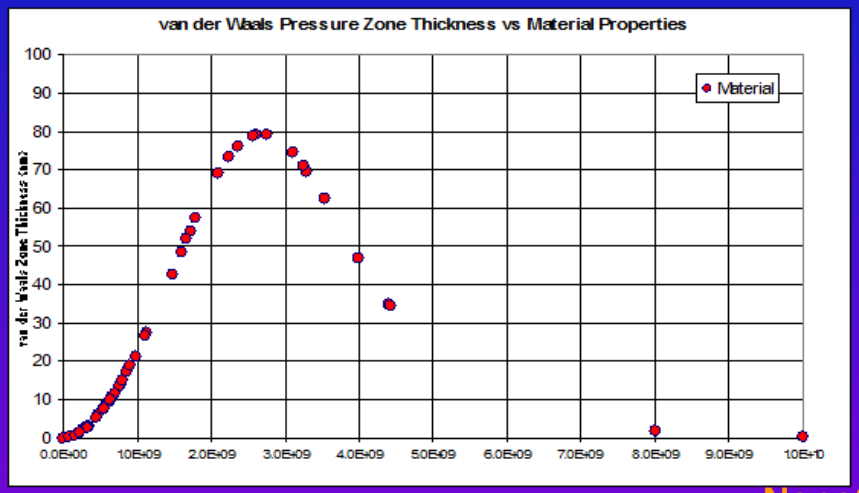

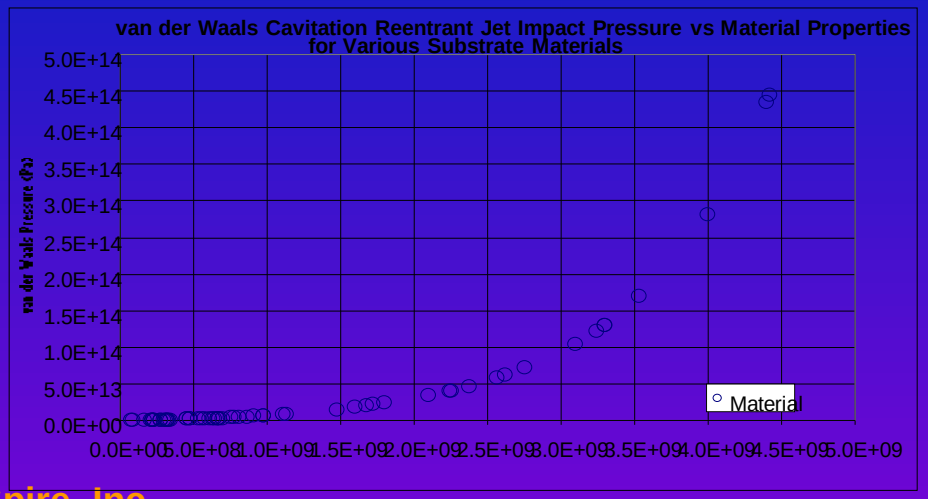

NanoSpire Redefines Cavitation Erosion Prediction State of the Art:

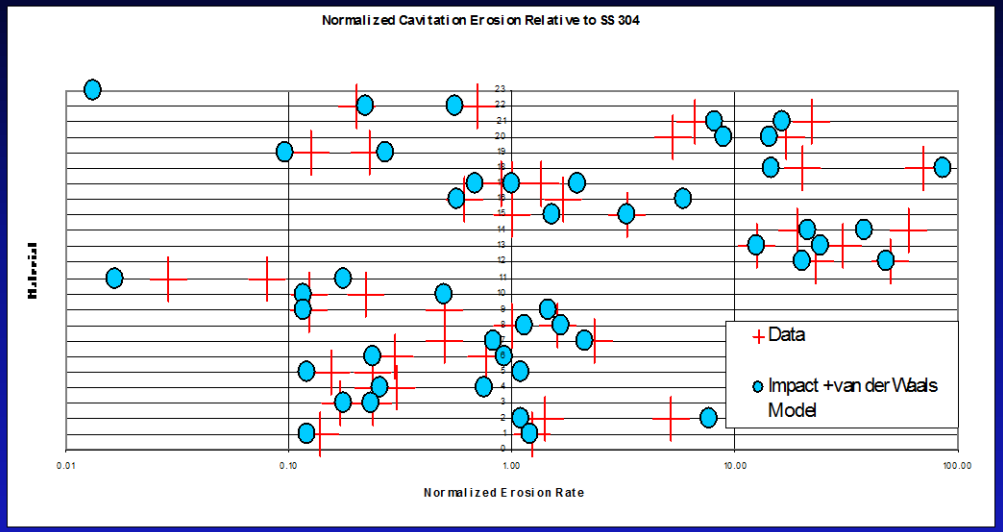

Charts Show NanoSpire Cavitation Erosion Prediction vs. Data for 22 Different Materials, Including Pure Metals, Alloys, Ceramics, Glass & Other Materials. Top Chart Shows Normalized Cavitation Erosion Resistance Rate Prediction (Blue Dots) vs. Data for Typical Hardness Range within Red Bars for a Given Substance. Lower Chart Shows Prediction has a 98% R^2 Fit With Data.

"Even elaborate correlations often err by as much as 300%, and for untested materials may predict erosion rates that are in error by an order of magnitude or more from the actual rate determined by subsequent testing. From Liquid Erosion Failures, Metals Handbook, vol. 10, 1975."

"The resistance of specific metals or other materials to liquid erosion, which is commonly evaluated by ASTM G32(Standard Method for Vibratory Cavitation Erosion Test), ***does not depend on any one property***, although many attempts have been made to correlate erosion damage with different intrinsic properties … hardness, true stress at fracture, corrosion fatigue strength, work hardening rate and ultimate resilience (one half the square of the ultimate strength, divided by the modulus of elasticity. From Liquid Erosion Failures, Metals Handbook, vol. 10, 1975."

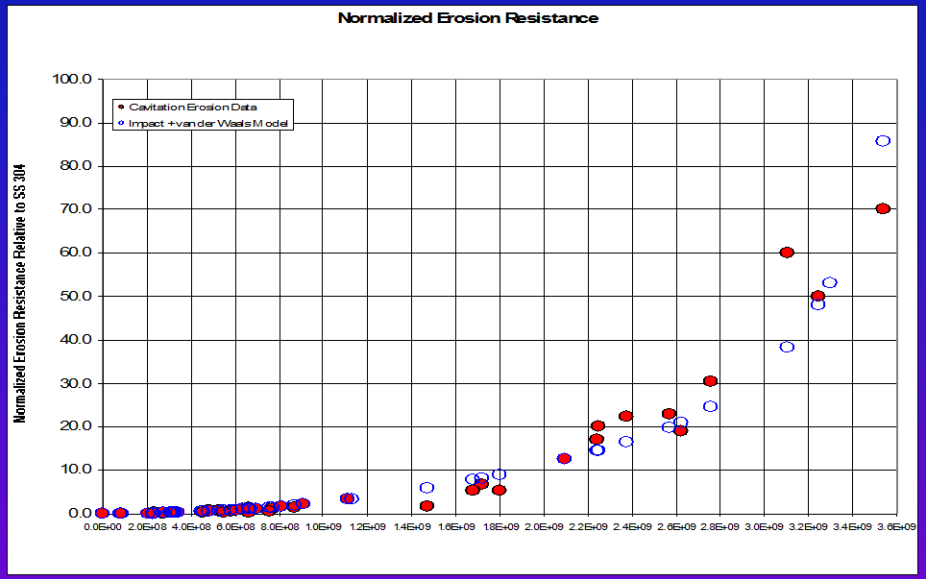

10/20/2012

NanoSpire, Inc.

Faceted Cavitation Reentrant Jet Impact Pits

Photo: L. A. Crum

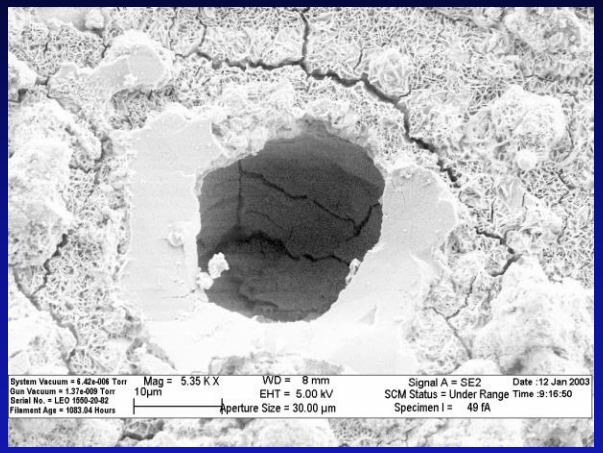

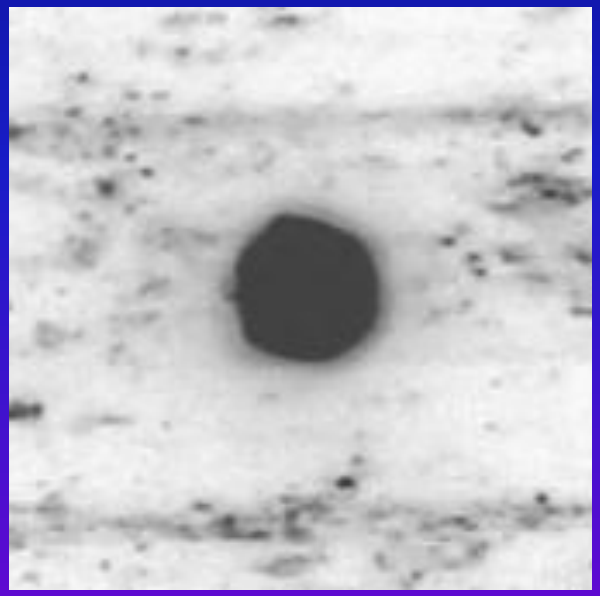

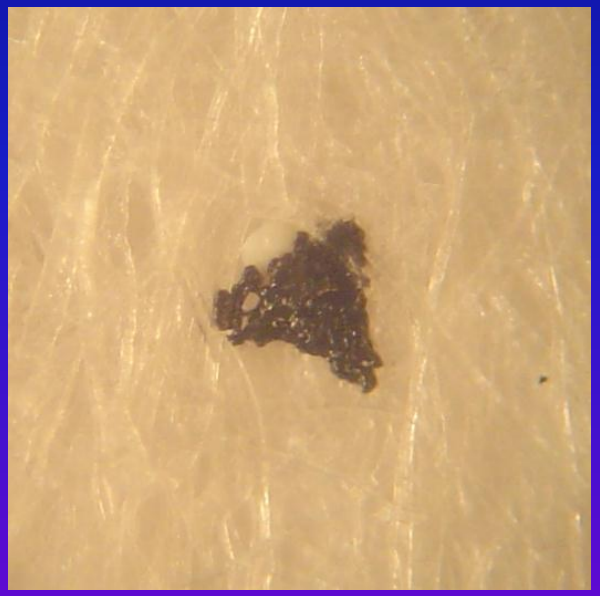

First Examples of the LeClair Effect 2/19/04

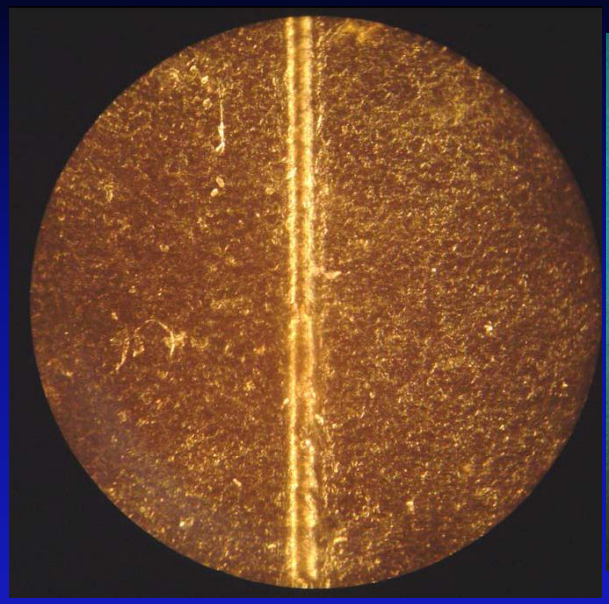

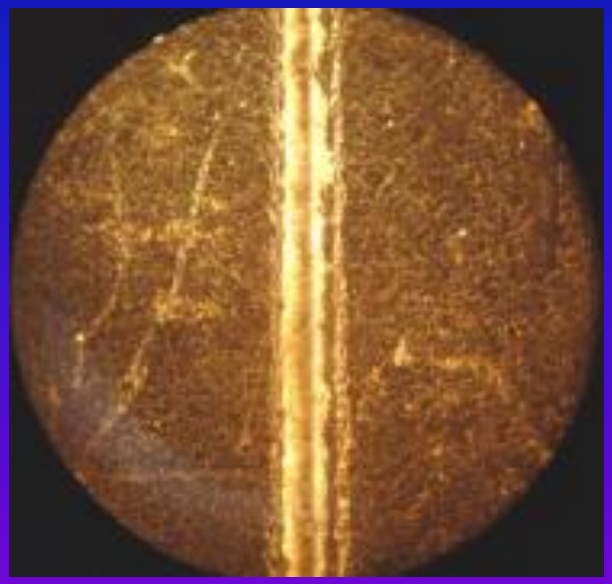

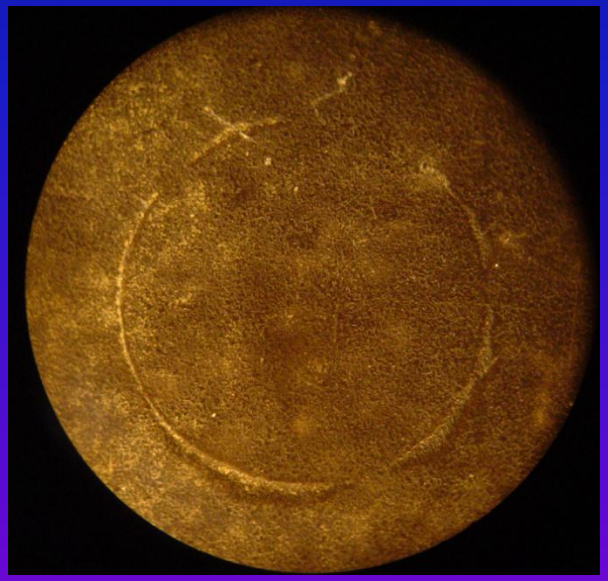

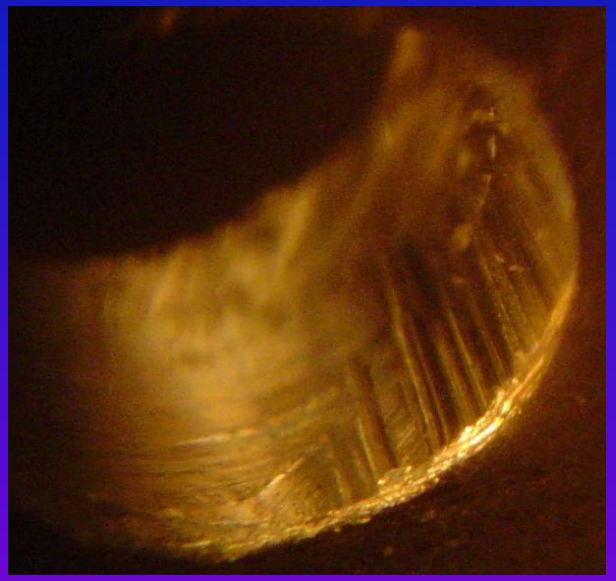

10/20/2012

NanoSpire, Inc.

The Water Crystal

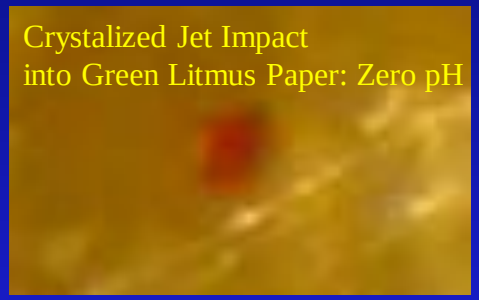

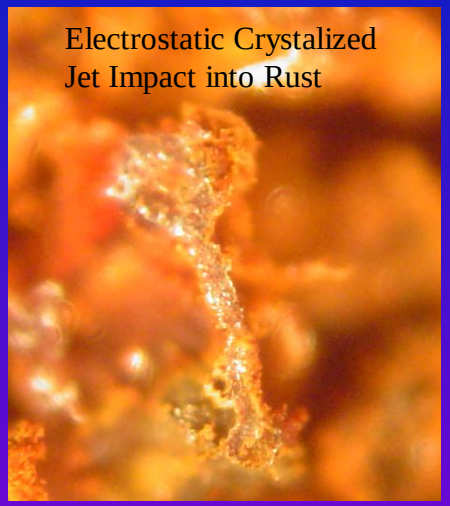

NanoSpire, Inc.

Cavitation Water Crystal Molecular Structure & Proposed Brown's Gas Seed

Water Crystal Discovered by Mark L. LeClair, 2004.

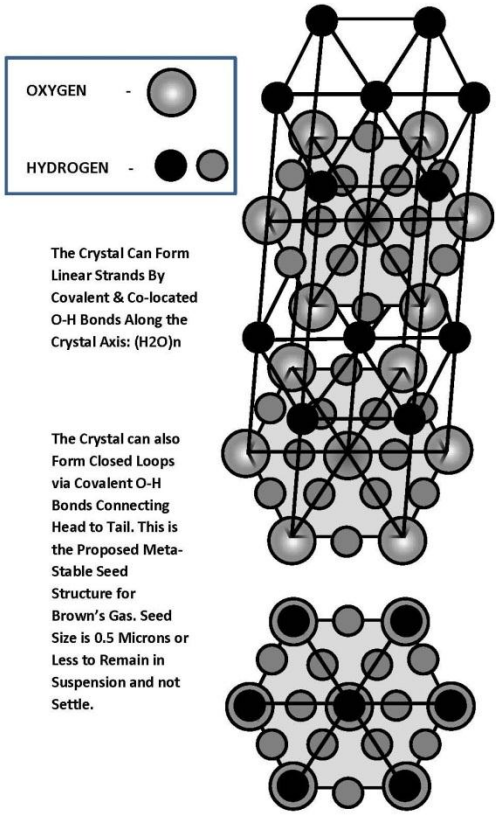

The Crystal Can Form Linear Strands By Covalent & Co-located O-H Bonds Along the Crystal Axis: $(H_2O)_n$

The Crystal can also Form Closed Loops via Covalent O-H Bonds Connecting Head to Tail. This is the Proposed Meta-Stable Seed Structure for Brown's Gas. Seed Size is 0.5 Microns or Less to Remain in Suspension and not Settle.

The Crystal Subunit is an Equilateral Triangle. These can Link Into Hexagons and Larger Structures, Bound Together in the Plane by Either Weak Hydrogen Bonds or Co-located Hydrogen Atoms. A Combination of O-H Covalent Bonds along the Axis with Hydrogen Bonds in the Plane Classifies the Water Crystal as a Hybrid, a Type of Van der Waals Crystal. The Specific Gravity can Vary: Ranging From 5.5 Max for the All Co-located Hydrogen Case Down to 0.73 for the Case where the Bonds Alternate Between O-H Covalent (0.19 nm) and Hydrogen Bonds (0.28 nm) in All Directions. The Crystal is not a Form of Ice, Forming at the Ultra High Pressures of Cavitation Collapse and Reentrant Jet Impact

The Crystal Loop Can Break, The LeClair Effect Then Accelerates the Strand, Releasing Zero Point Energy & Can Trigger Nuclear Reactions Ahead of the Crystal's Supersonic Bow Shock

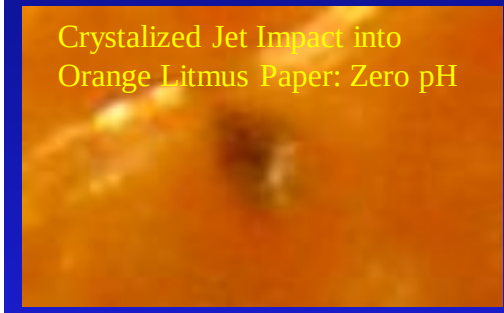

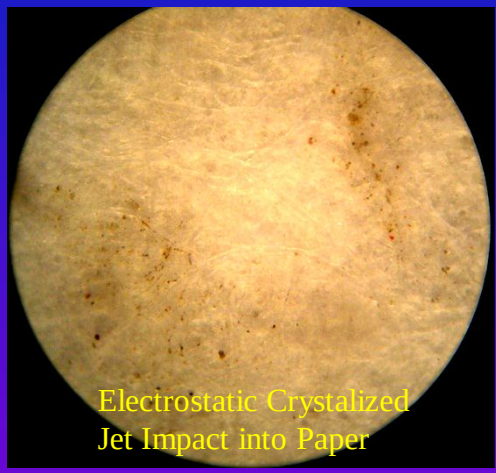

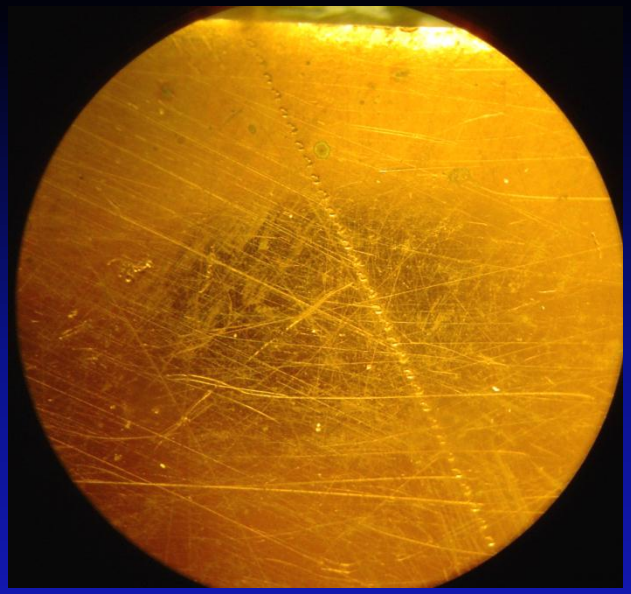

Spiraling LeClair Effect Crystalized Reentrant Jet Trenches on Copper

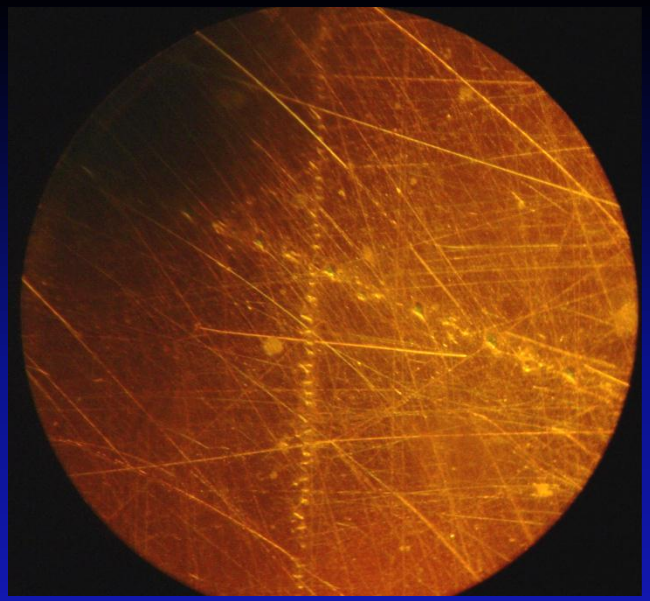

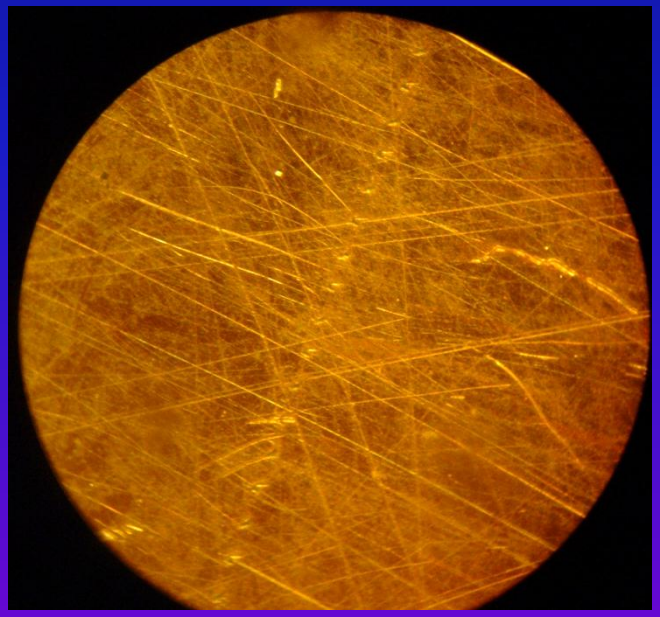

The LeClair Effect

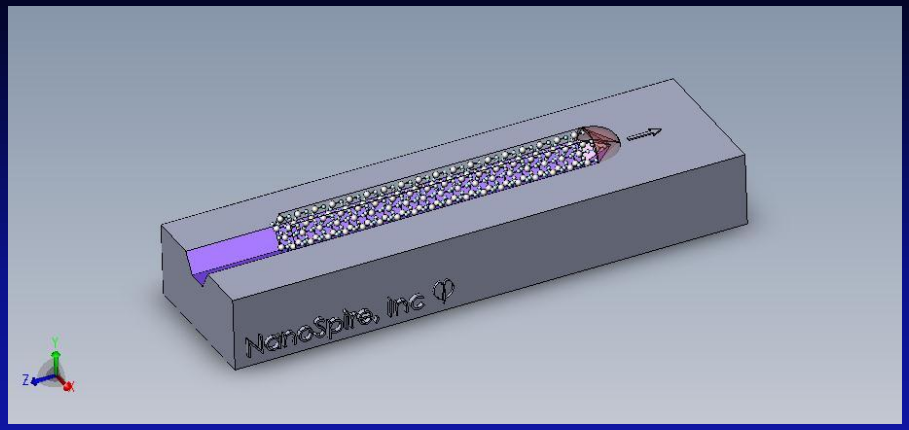

The leading face of the highly charged crystal and bow shock are in sub-micron proximity, their closely spaced conductive faces, separated by a near vacuum, satisfy the conditions for forming a resonant quantum harmonic oscillator, producing the Casimir force. The Casimir force, along with electrostatic attraction, cause the bow shock to draw the crystal towards it, this propels the crystal. The Casimir force coherently extracts zero point energy as a result of the zero point electron cloud positional fluctuation of the closely spaced conductive surfaces. The highly fixed particle positions pinned on the bow shock from high pressure invoke the Heisenberg Uncertainty Principal, which then imposes random, zero point momentum fluctuations of the electrons and other particles on the bow shock. Forced to respond with random momentum by the Heisenberg Uncertainty Principal, the highly fixed position bow shock particles can not respond with an equal and opposite reaction, thereby conflicting with Newton's Law's of Motion and violating the First and Second Laws of Thermodynamics

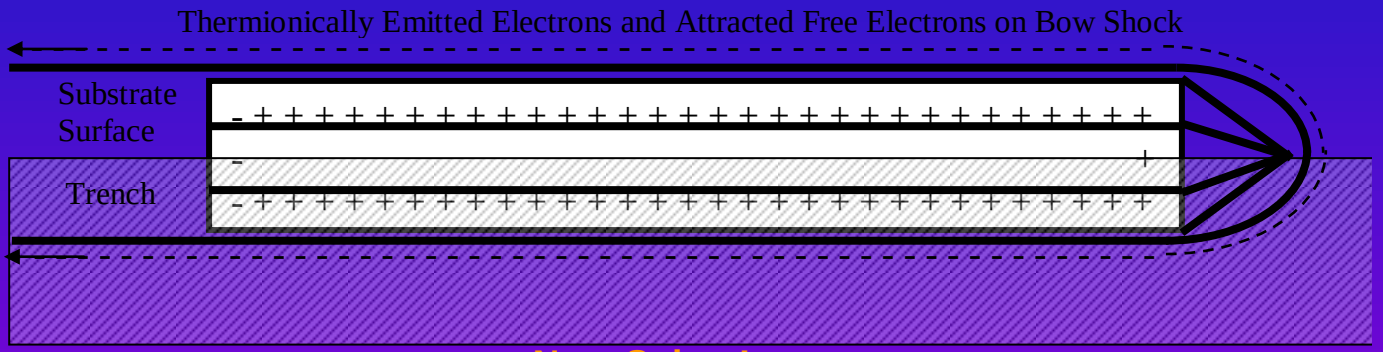

First LeClair Effect Cavitation Zero Point Energy (ZPE) Reactor Experiments 3/8/2007 -3/19/2007

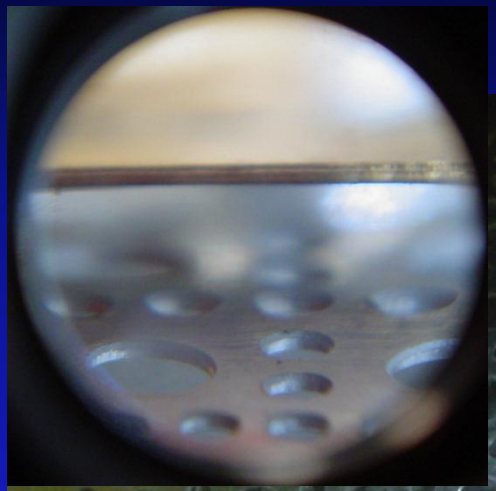

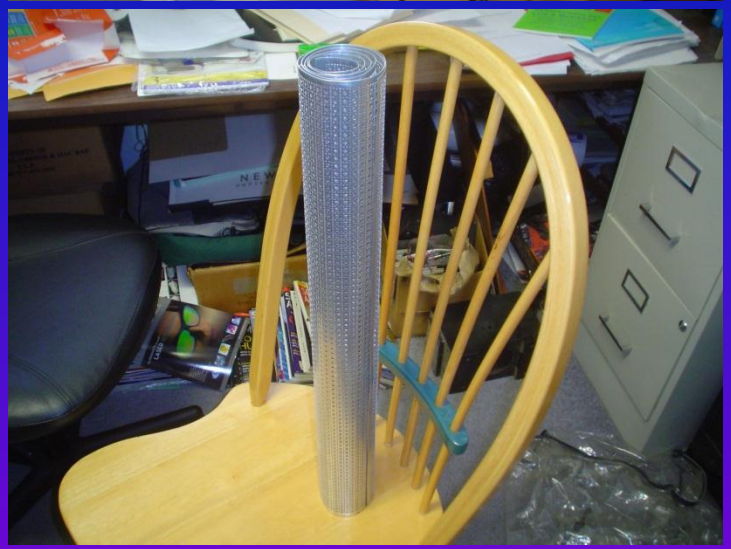

July 22, 2009 Cavitation ZPE Reactor Experiments

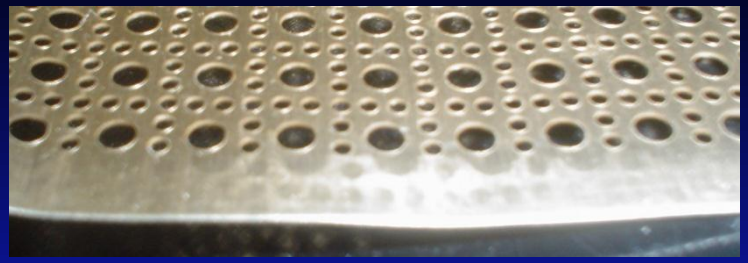

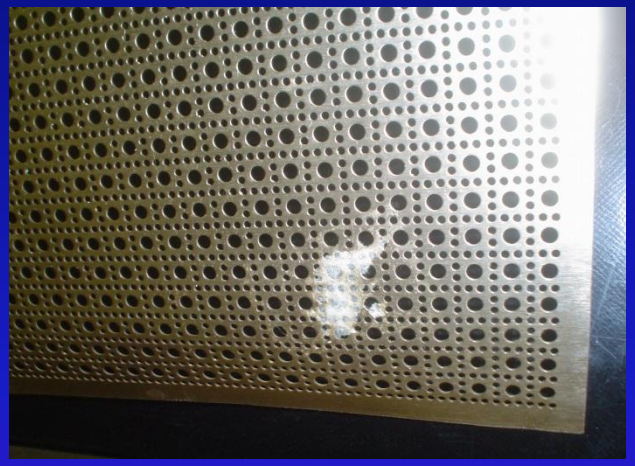

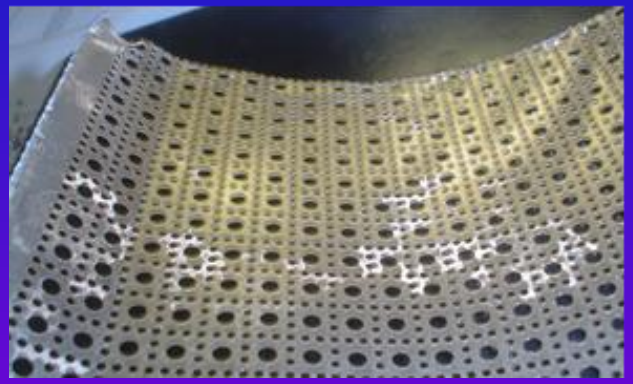

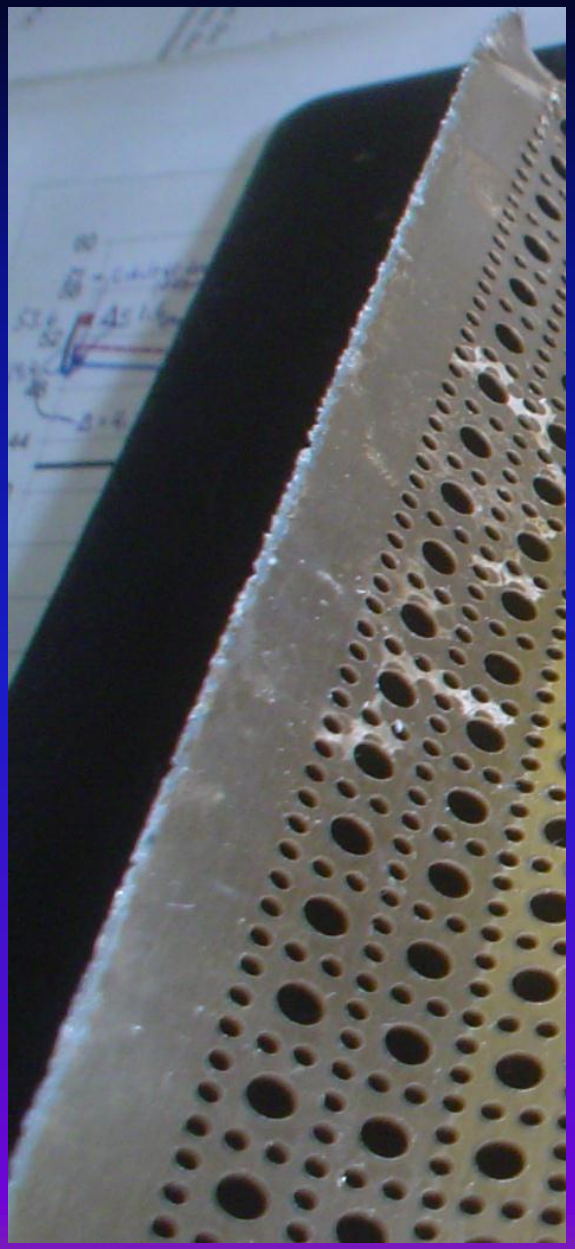

Majority of Transmuted Material was Diamond

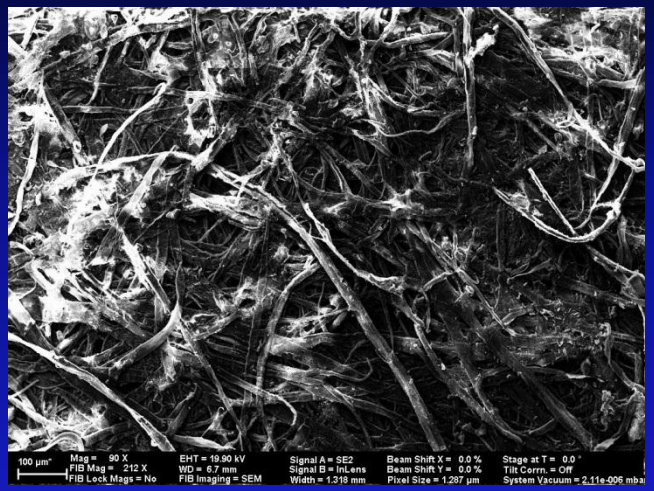

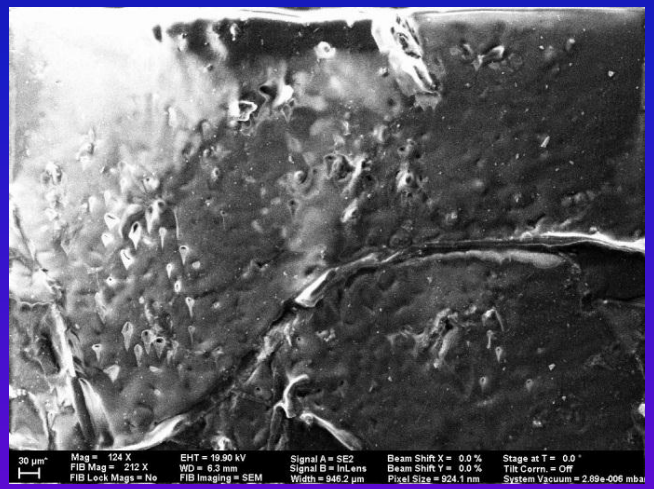

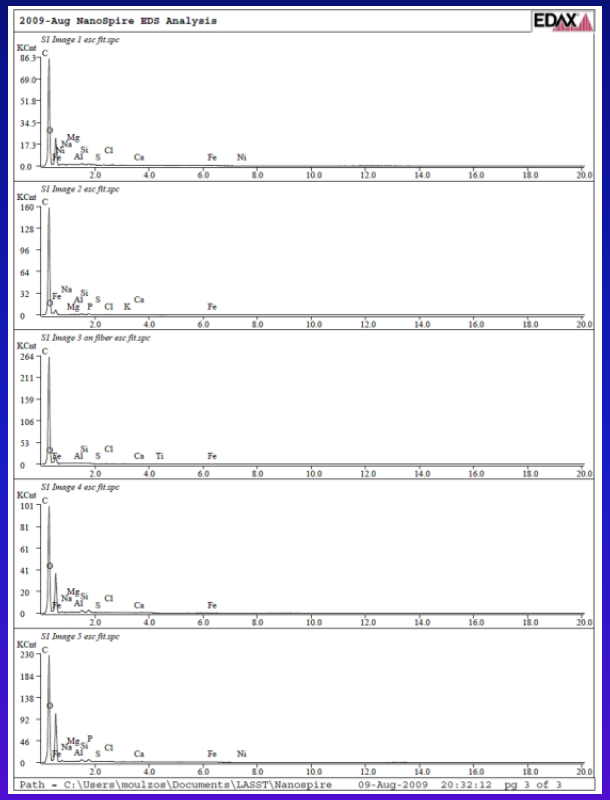

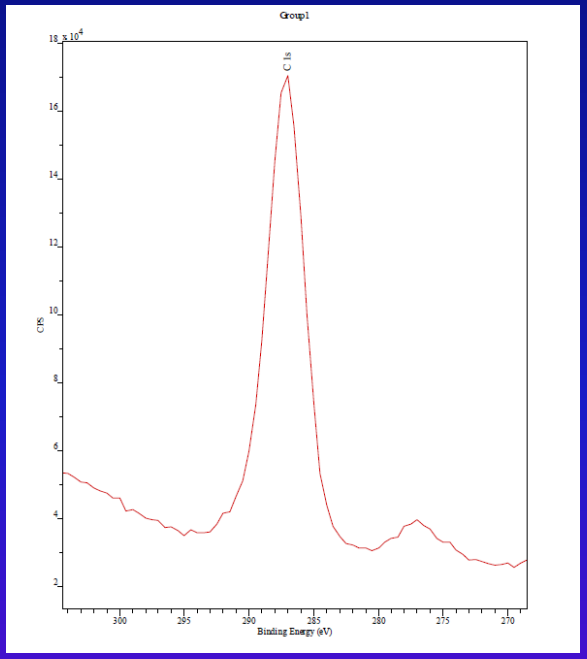

August 24-25, 2009
Cavitation ZPE Reactor Experiments

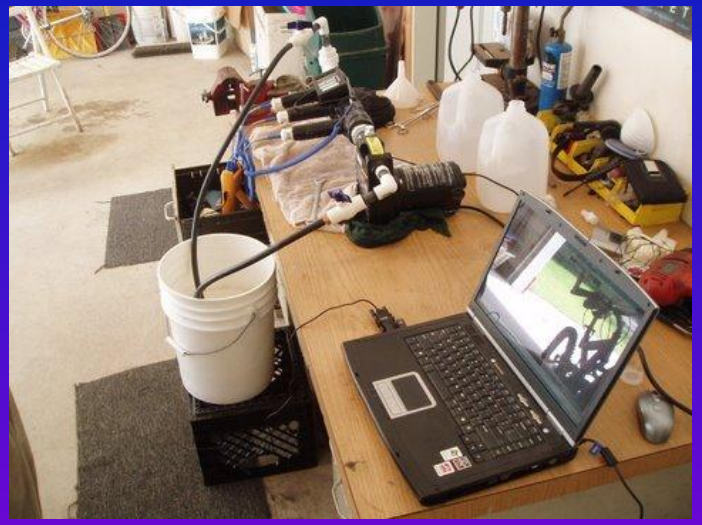

April 12, 2010 NRL Cavitation Reactor Experiment

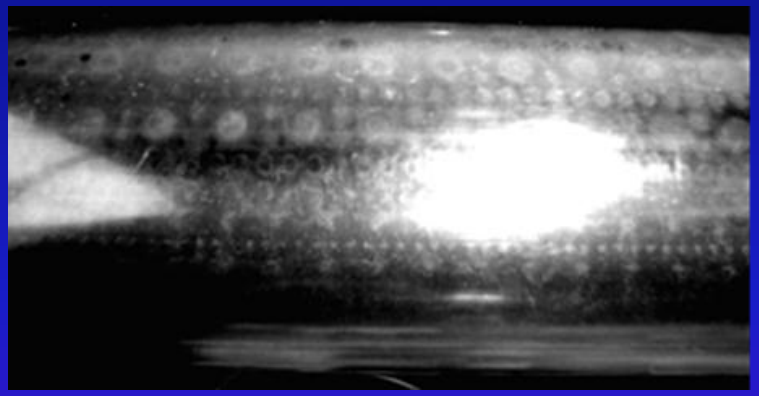

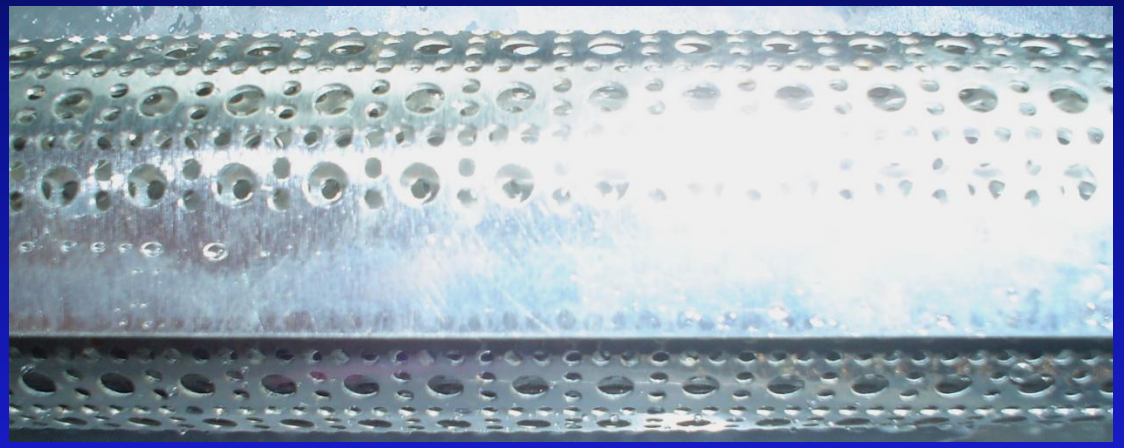

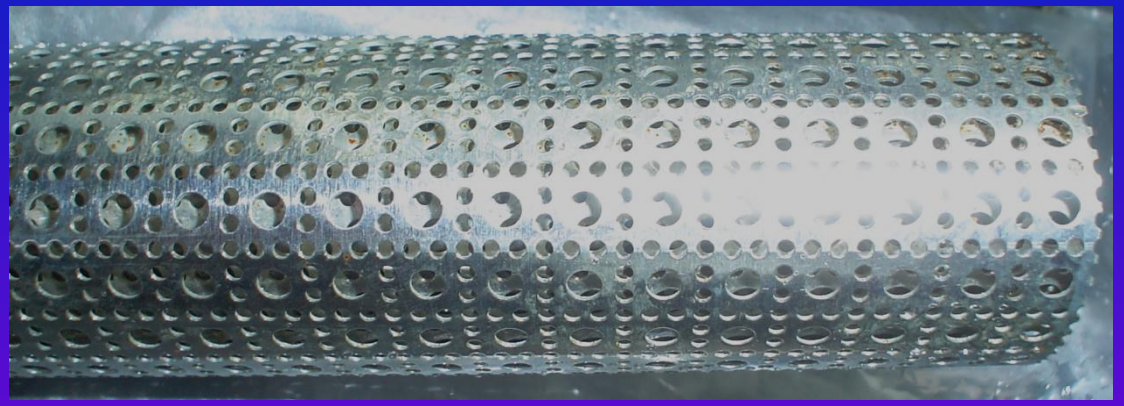

NanoSpire, Inc.

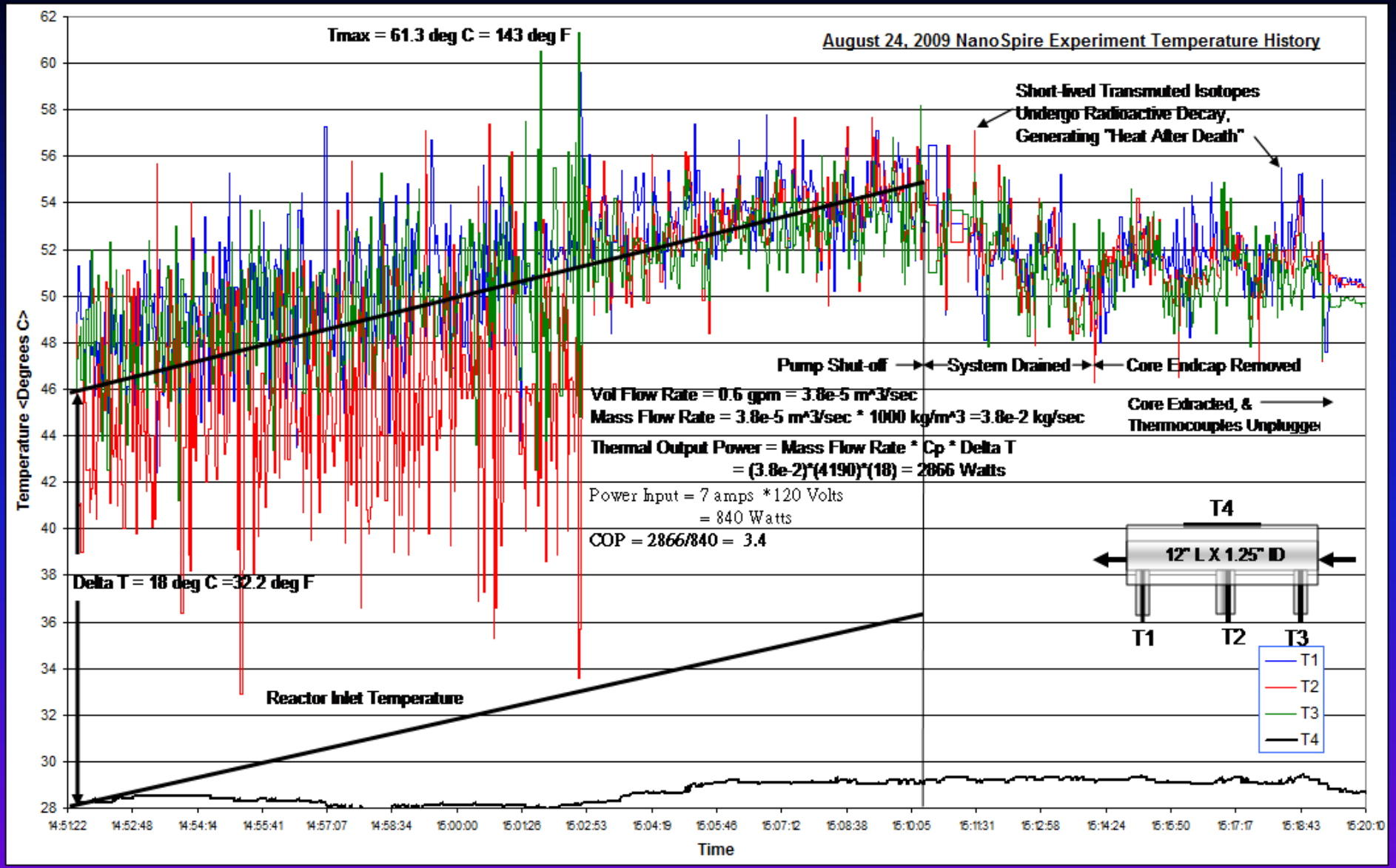
August 24, 2009 NanoSpire Experiment Temperature History
Tmax = 61.3 deg C = 143 deg F
Short-lived Transmuted Isotopes
Undergo Radioactive Decay,
Generating "Heat After Death"
Pump Shut-off
System Drained
Core Endcap Removed
Vol Flow Rate = 0.6 gpm = 3.8e-5 m^3/sec
Mass Flow Rate = 3.8e-5 m^3/sec * 1000 kg/m^3 =3.8e-2 kg/sec
Core Extracted, &
Thermocouples Unplugge
Thermal Output Power = Mass Flow Rate * Cp * Delta T
= (3.8e-2)*(4190)*(18) = 2866 Watts
Power Input = 7 amps *120 Volts
= 840 Watts
COP = 2866/840 = 3.4
Delta T = 18 deg C =32.2 deg F
Reactor Inlet Temperature
T4
12" L X 1.25" ID
T1
T2
T3
T1
T2
T3
T4
Temperature <Degrees C>
Time

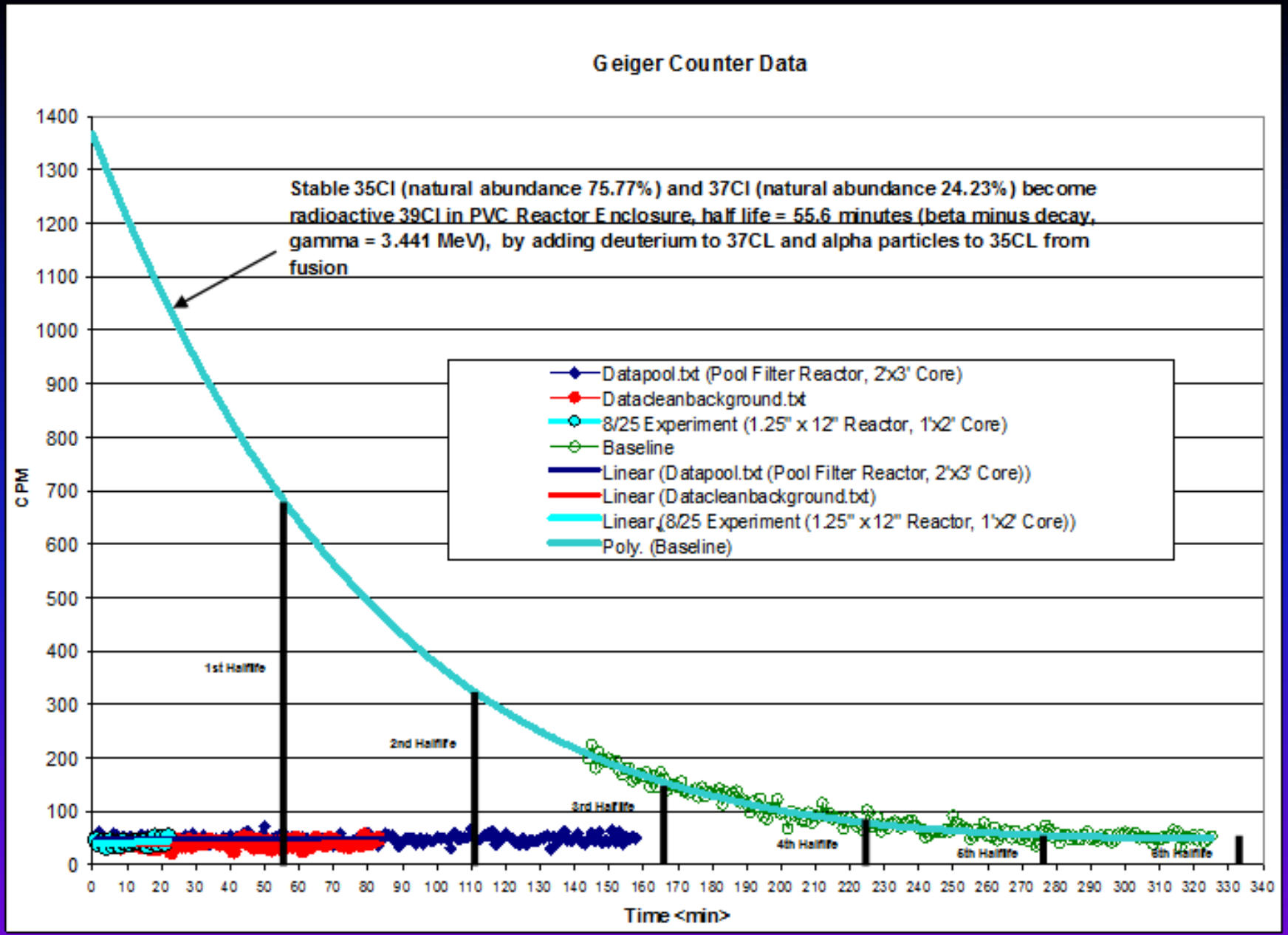
Geiger Counter Data
Stable 35Cl (natural abundance 75.77%) and 37Cl (natural abundance 24.23%) become radioactive 39Cl in PVC Reactor Enclosure, half life = 55.6 minutes (beta minus decay, gamma = 3.441 MeV), by adding deuterium to 37CL and alpha particles to 35CL from fusion
Datapool.txt (Pool Filter Reactor, 2'x3' Core)
Datacleanbackground.txt
8/25 Experiment (1.25" x 12" Reactor, 1'x2' Core)
Baseline
Linear (Datapool.txt (Pool Filter Reactor, 2'x3' Core))
Linear (Datacleanbackground.txt)
Linear (8/25 Experiment (1.25" x 12" Reactor, 1'x2' Core))
Poly. (Baseline)
1st Halflife
2nd Halflife
3rd Halflife
4th Halflife
5th Halflife
6th Halflife
CPM
Time <min>

Nuclear Tracks from Transmuted Material

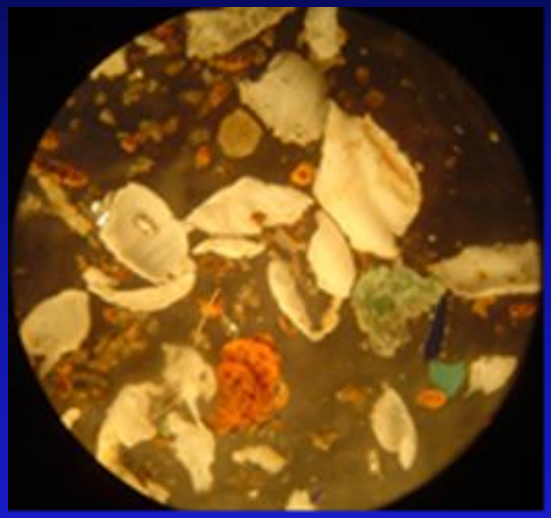

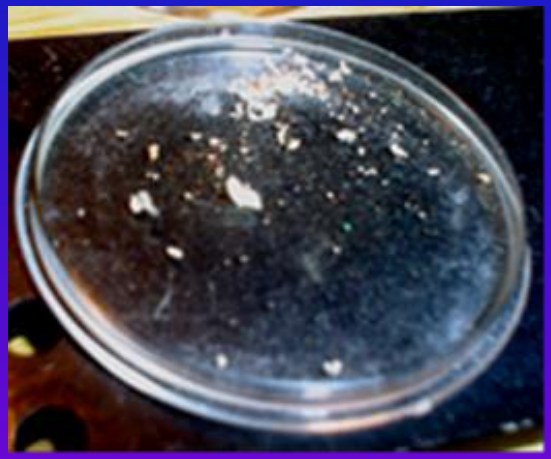

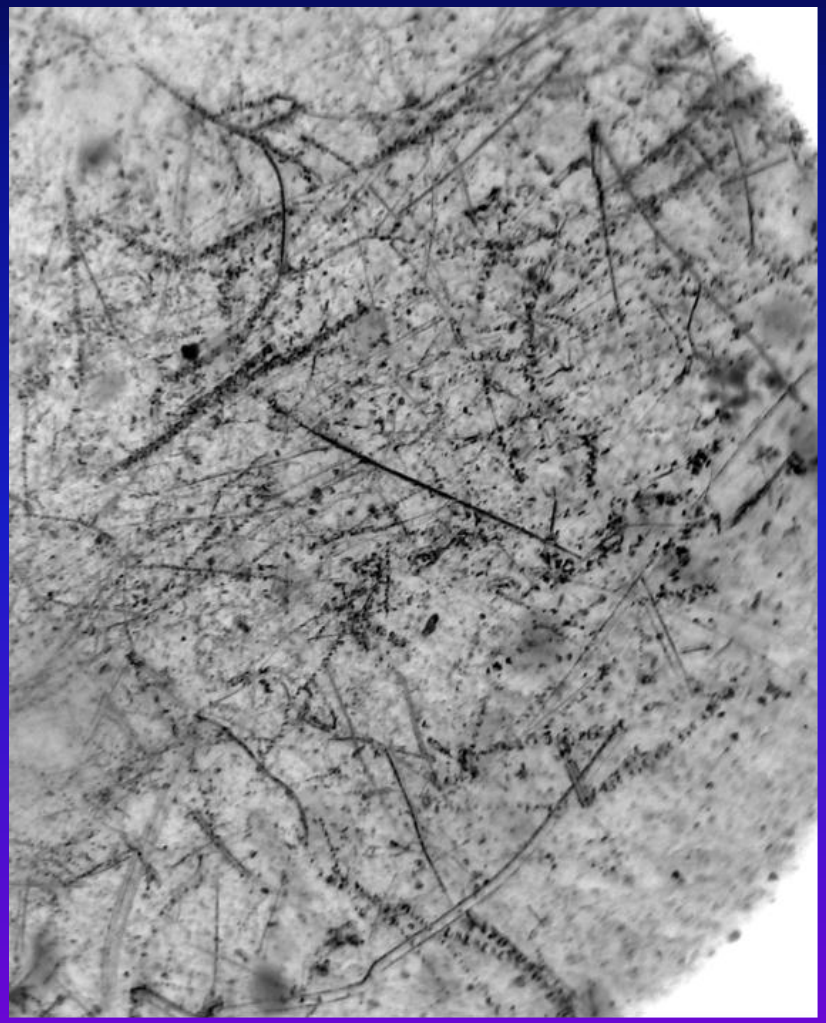

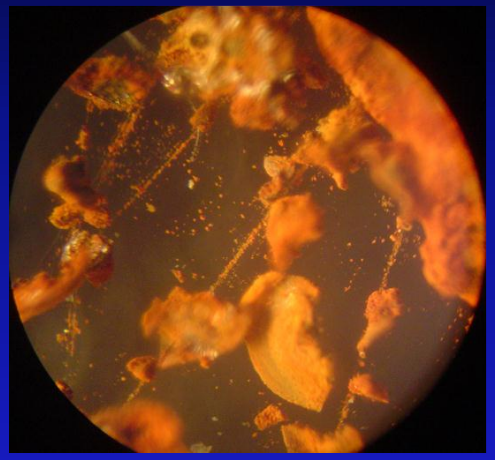

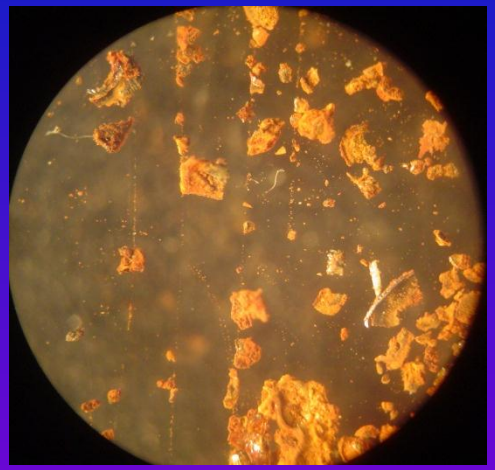

Blue Chip

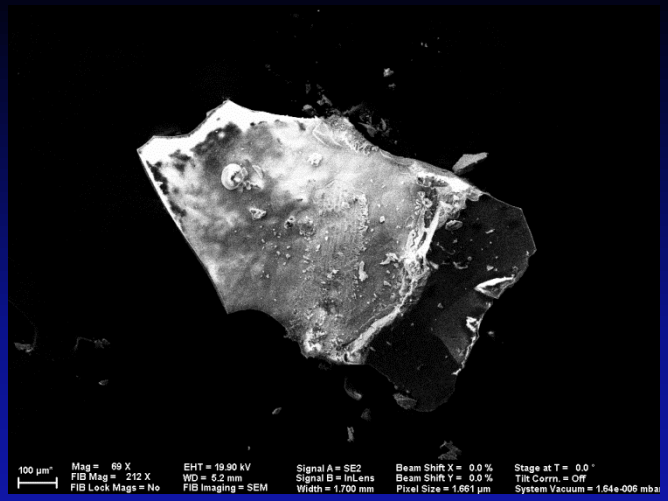

Transmuted particles were analyzed by SEM-EDAX (U. ME Orono, Media Sciences and Dr. Ed Storms) XPS (U. ME Orono) and LA-ICP-MS (Evans Analytical)

Rust

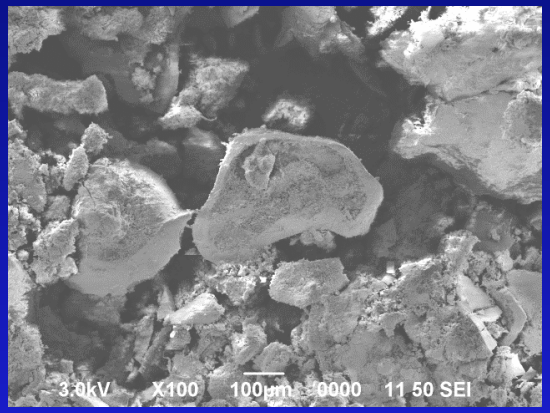

Conglomerate

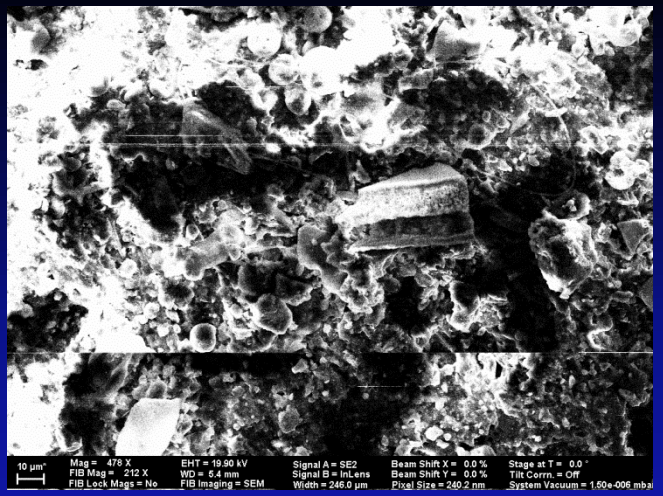

Orange Chip

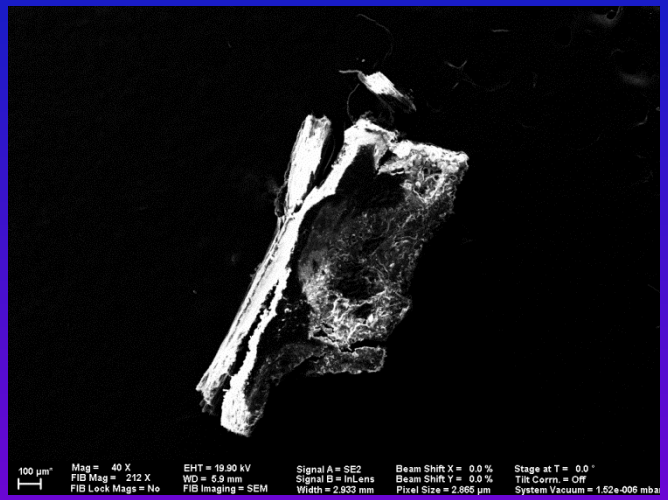

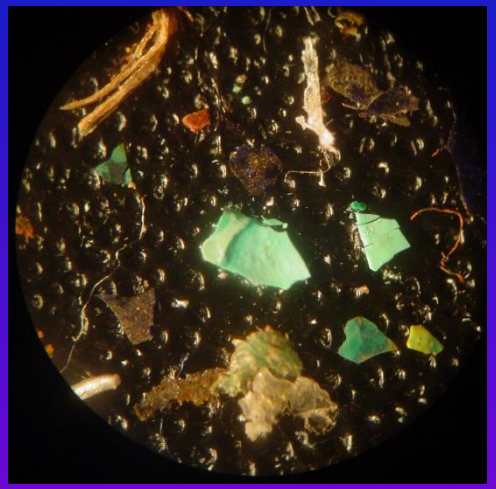

White Chip

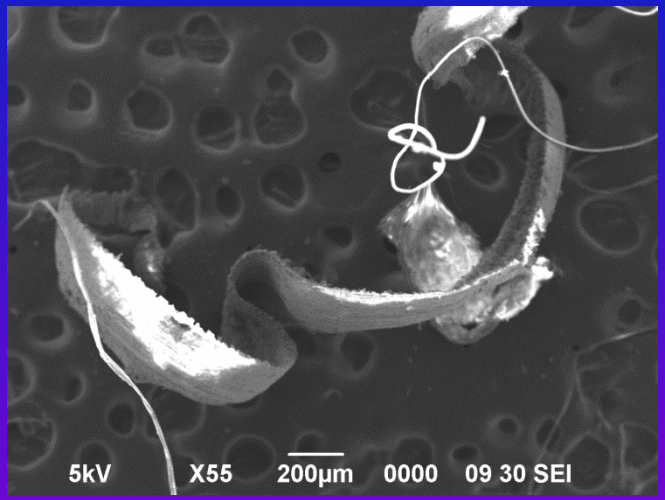

10/20/2012

NanoSpire, Inc.

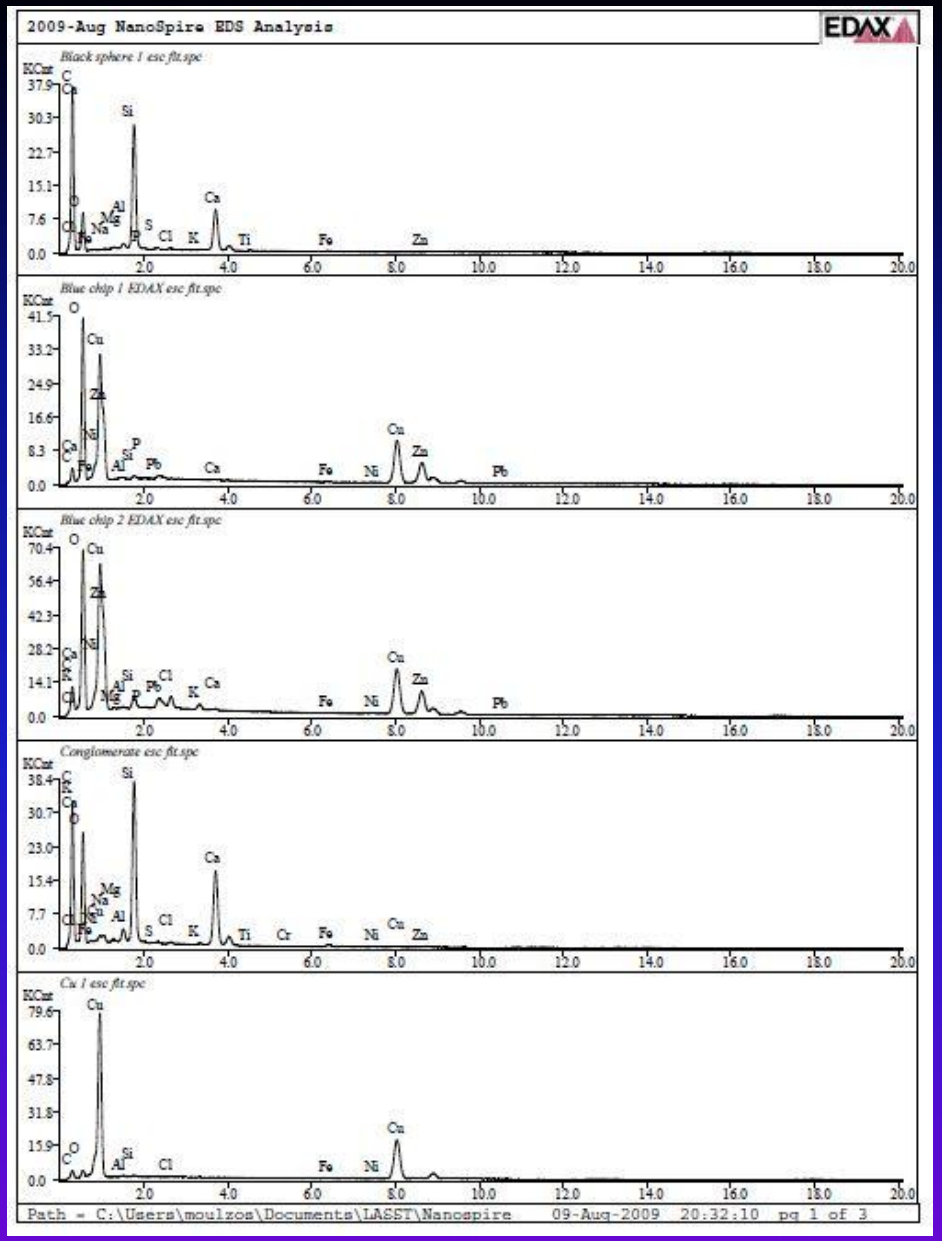
2009-Aug NanoSpire EDS Analysis
EDAX
Black sphere 1 esc flt.spc
Blue chip 1 EDAX esc flt.spc
Blue chip 2 EDAX esc flt.spc
Conglomerate esc flt.spc
Cu 1 esc flt.spc
KCnt
Path = C:\Users\moulzos\Documents\LASST\Nanospire 09-Aug-2009 20:32:10 pg 1 of 3

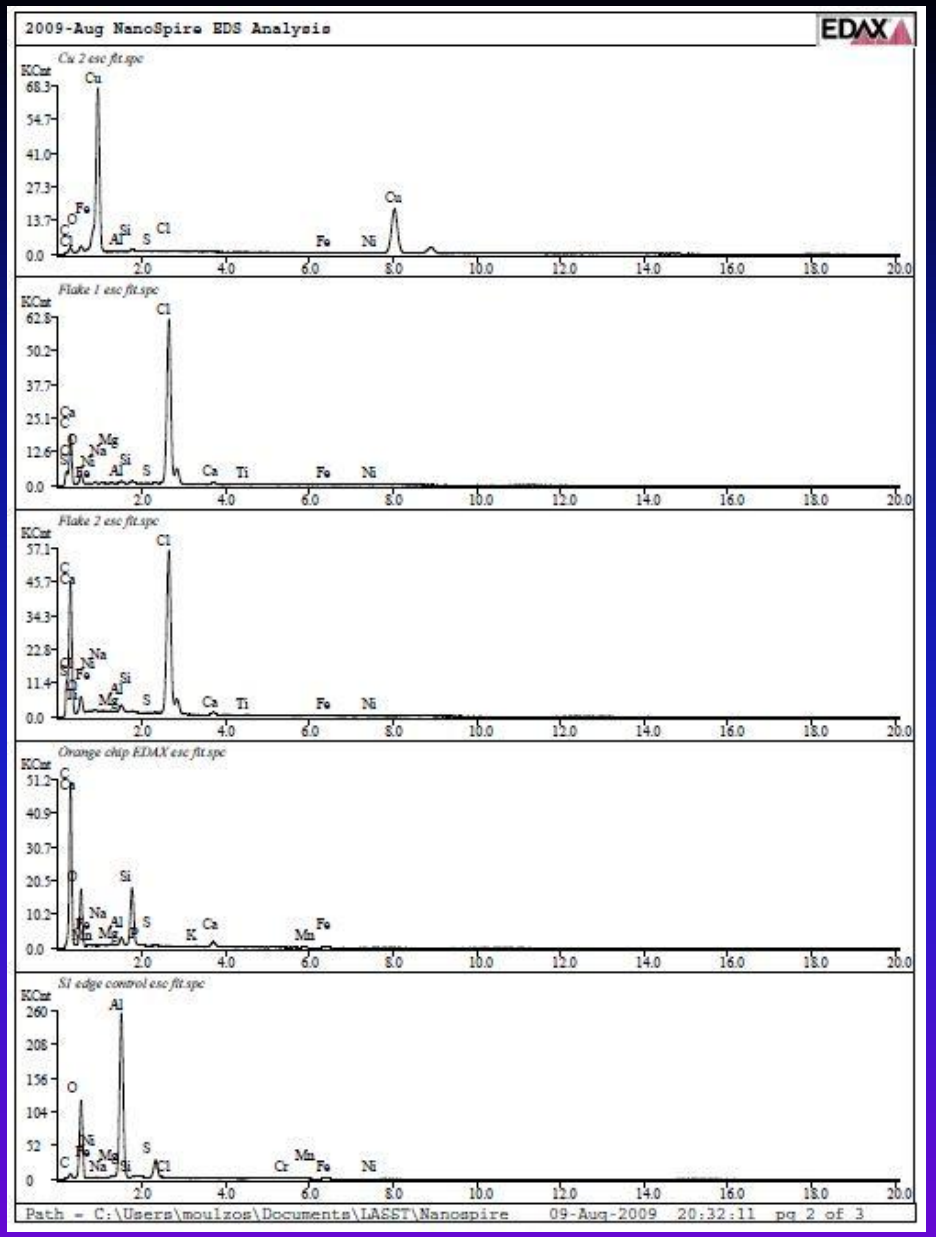
2009-Aug NanoSpire EDS Analysis
EDAX
Cu 2 esc flt.spc
Flake 1 esc flt.spc
Flake 2 esc flt.spc
Orange chip EDAX esc flt.spc
Si edge control esc flt.spc
KCnt
Path = C:\Users\moulzos\Documents\LASST\Nanospire 09-Aug-2009 20:32:11 pg 2 of 3

Transmuted Particle XPS Analysis (U ME)

NanoSpire Sample – Perforated Al sheet with white deposit

The nanospire sample was analyzed using XPS. The power was 240 W (12 kV at 20 mA) using the Al anode. All scans were done at 100 eV pass energy for high S/N. The sample was placed on a piece of silicon; due to the perforations in the sample and the large analysis area, the silicon sample contributed peaks to the spectrum. Several scans were taken. The sample definitely contains carbon, oxygen, sulfur, nitrogen and aluminum. Two silicon peaks were seen – one from the silicon piece and the other from the native silicon oxide on the piece or the sample. The wide scan below shows silicon, aluminum, oxygen, and carbon.

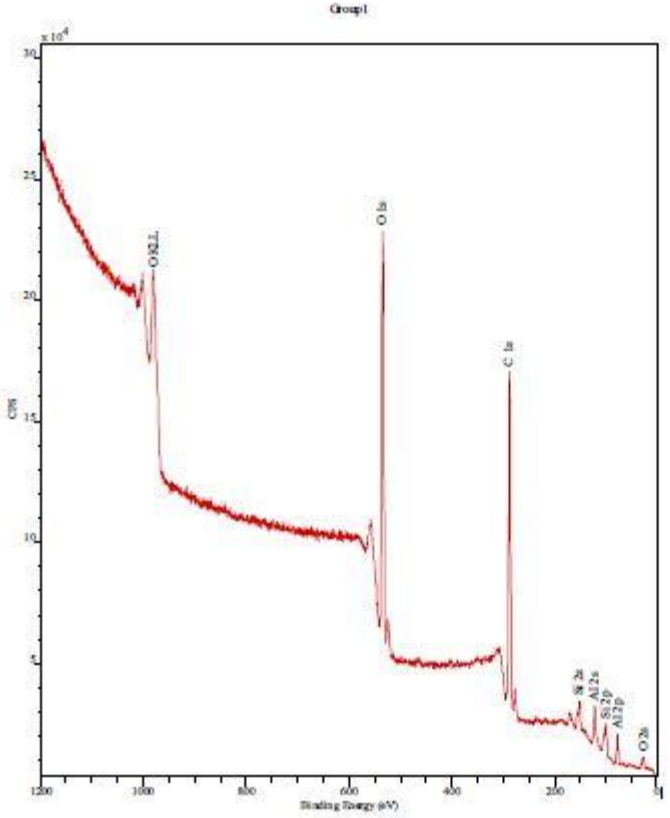

The most populated region showed a variety of peaks.

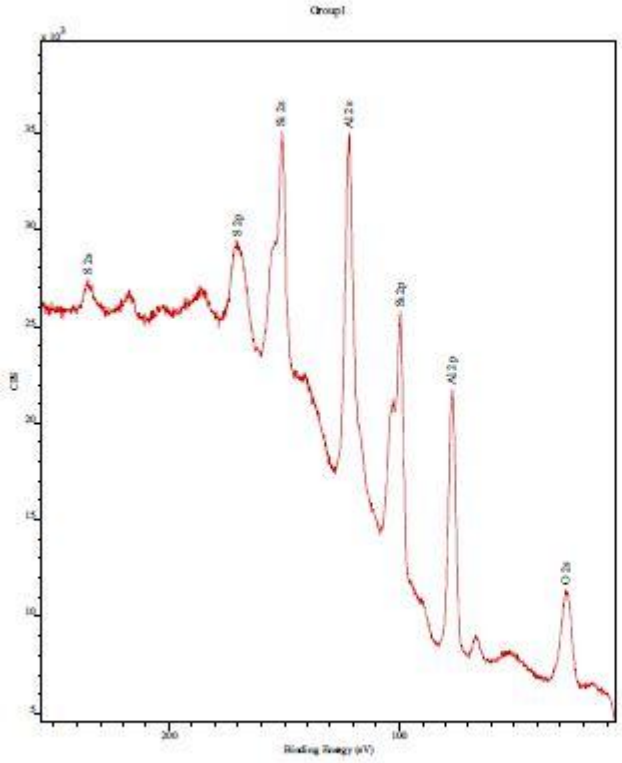

Here you can clearly see the aluminum, silicon (double state) and sulfur. The other unknown peaks are possibly chlorine or boron.

Orange Chip

Isotope	Intensity cps	Element	Intensity cps
Li7	386	Cd114	2564
Be9	3	In115	289
B10	17873	Sn117	23939
B11	17568	Sn118	29449
Na23	918027	Sb121	1873
Mg24	1694854	Sb123	2756
Mg25	1806485	Te125	14566
Al27	4775204	Te128	14216
Si28	10881596	Cs133	1197
Si29	10185407	Ba135	2080052
P31	84503	Ba137	1829746
K39	828438	La139	21810
Ca43	107246222	Ce140	16329
Ca44	63131879	Ce142	41909
Sc45	0	Pr141	2747
Ti47	28592	Nd146	8242
Ti49	26632	Pm147	160
V51	4756	Sm147	1067
Cr52	174012	Eu153	384
Cr53	33581	Gd157	1107
Mn55	4387305	Tb159	167
Fe56	1644305	Dy163	869
Fe57	1495591	Ho165	214
Co59	1176	Er166	347
Ni60	15164	Tm169	44
Ni62	18475	Yb172	290
Cu63	43440	Lu175	21
Cu65	43359	Hf177	610
Zn66	140498	Hf178	629
Zn67	146951	Ta181	40
Ga69	20686	W182	596
Ga71	6803	W183	306
Ge72	0	Re185	0
Ge73	0	Os189	0
As75	473	Ir193	5
Se77	487	Pt194	5157
Se82	386	Pt195	5770
Rb85	12114	Au197	3
Sr87	1178436	Hg201	4590
Sr88	1086860	Hg202	7273
Y89	5641	Tl205	672
Zr90	12400	Pb206	67927
Zr91	13561	Pb208	62549
Nb93	747	Bi209	603
Mo95	6512	Po210	14
Mo97	2866	Th232	447
Ru101	0	Pa231	0
Rh103	0	U238	584
Pd105	0	Np237	0
Pd106	0	Pu239	34
Ag107	0	Am241	10
Ag109	0	Cm245	0
Cd111	2213	Bk247	0
Cd113	1557	Cf249	0

Blue Chip

Isotope	Intensity cps	Element	Intensity cps
Li7	0	Cd114	291711
Be9	0	In115	26953
B10	3732	Sn117	5882411
B11	3806	Sn118	6023267
Na23	2194	Sb121	388743
Mg24	63854	Sb123	400688
Mg25	68541	Te125	10641
Al27	41252	Te128	12786
Si28	317096	Cs133	0
Si29	394229	Ba135	13996
P31	2731	Ba137	13572
K39	121703	La139	36
Ca43	3600593	Ce140	36
Ca44	3922291	Ce142	62
Sc45	0	Pr141	0
Ti47	0	Nd146	0
Ti49	396	Pm147	0
V51	61	Sm147	17
Cr52	1068	Eu153	0
Cr53	661	Gd157	0
Mn55	107683	Tb159	0
Fe56	12677	Dy163	10
Fe57	11523	Ho165	3
Co59	6046	Er166	0
Ni60	861914	Tm169	0
Ni62	962579	Yb172	0
Cu63	480736552	Lu175	3
Cu65	605699405	Hf177	0
Zn66	449023774	Hf178	0
Zn67	438655939	Ta181	0
Ga69	5229	W182	15908
Ga71	5123	W183	16820
Ge72	2287	Re185	115
Ge73	4512	Os189	0
As75	2587	Ir193	0
Se77	1366	Pt194	8
Se82	0	Pt195	0
Rb85	649	Au197	12
Sr87	103064	Hg201	0
Sr88	105474	Hg202	0
Y89	0	Tl205	3330
Zr90	26	Pb206	136290921
Zr91	463	Pb208	139834167
Nb93	23	Bi209	6196
Mo95	3351	Po210	0
Mo97	3840	Th232	0
Ru101	0	Pa231	3
Rh103	243884	U238	2528
Pd105	20	Np237	3
Pd106	279020	Pu239	21
Ag107	21656	Am241	1
Ag109	277	Cm245	18
Cd111	162988	Bk247	79
Cd113	161003	Cf249	0

Conglomerate

Isotope	Intensity cps	Element	Intensity cps
Li7	480	Cd114	5853
Be9	8	In115	1387
B10	756	Sn117	362293
B11	721	Sn118	359234
Na23	431952	Sb121	2618
Mg24	2011087	Sb123	2917
Mg25	2017220	Te125	23508
Al27	1497543	Te128	24944
Si28	49376451	Cs133	557
Si29	49663062	Ba135	223870
P31	6065	Ba137	194394
K39	224136	La139	10484
Ca43	69782074	Ce140	27281
Ca44	67341802	Ce142	33987
Sc45	1824	Pr141	2655
Ti47	292732	Nd146	6997
Ti49	312991	Pm147	175
V51	10502	Sm147	1165
Cr52	44781	Eu153	345
Cr53	17614	Gd157	1305
Mn55	47064	Tb159	146
Fe56	1427407	Dy163	804
Fe57	1514727	Ho165	198
Co59	974	Er166	524
Ni60	33009	Tm169	70
Ni62	32206	Yb172	408
Cu63	31003	Lu175	39
Cu65	46711	Hf177	687
Zn66	178850	Hf178	739
Zn67	215417	Ta181	55
Ga69	6837	W182	660
Ga71	4031	W183	390
Ge72	0	Re185	345
Ge73	0	Os189	99
As75	721	Ir193	2
Se77	0	Pt194	93
Se82	0	Pt195	379
Rb85	5429	Au197	3488
Sr87	1636017	Hg201	0
Sr88	1534267	Hg202	0
Y89	4106	Tl205	99
Zr90	18244	Pb206	229605
Zr91	18958	Pb208	363492
Nb93	611	Bi209	633
Mo95	1013	Po210	0
Mo97	1510	Th232	583
Ru101	15	Pa231	12
Rh103	0	U238	15675
Pd105	0	Np237	0
Pd106	166	Pu239	12
Ag107	23647	Am241	16
Ag109	28293	Cm245	6
Cd111	4863	Bk247	0
Cd113	4977	Cf249	0

White Chip

Isotope	Intensity cps	Element	Intensity cps
Li7	0	Cd114	1776718
Be9	3	In115	128
B10	0	Sn117	69715544
B11	6	Sn118	68964067
Na23	77239	Sb121	824
Mg24	207466	Sb123	1340
Mg25	248121	Te125	23487
Al27	255464	Te128	24031
Si28	24114	Cs133	155
Si29	32349	Ba135	14064
P31	3435	Ba137	11602
K39	98394	La139	2336
Ca43	128986963	Ce140	6508
Ca44	99367766	Ce142	13767
Sc45	0	Pr141	723
Ti47	48050407	Nd146	2863
Ti49	49066076	Pm147	67
V51	357	Sm147	445
Cr52	88367	Eu153	189
Cr53	13963	Gd157	921
Mn55	23609	Tb159	129
Fe56	1026232	Dy163	601
Fe57	1046482	Ho165	106
Co59	344	Er166	254
Ni60	4526	Tm169	64
Ni62	5696	Yb172	397
Cu63	21767	Lu175	65
Cu65	22900	Hf177	9083
Zn66	44704	Hf178	8197
Zn67	61234	Ta181	24
Ga69	636	W182	1034
Ga71	294	W183	842
Ge72	0	Re185	0
Ge73	0	Os189	0
As75	766	Ir193	4
Se77	1586	Pt194	0
Se82	1289	Pt195	0
Rb85	1135	Au197	15
Sr87	300671	Hg201	0
Sr88	315650	Hg202	0
Y89	2062	Tl205	32
Zr90	130364	Pb206	11022
Zr91	152619	Pb208	16154
Nb93	1160	Bi209	264
Mo95	387	Po210	0
Mo97	612	Th232	246
Ru101	31	Pa231	0
Rh103	12	U238	488
Pd105	18	Np237	15
Pd106	0	Pu239	16
Ag107	67	Am241	0
Ag109	0	Cm245	5
Cd111	1519	Bk247	14
Cd113	972	Cf249	18

Rust

Isotope	Intensity cps	Element	Intensity cps
Li7	292	Cd114	9227
Be9	10	In115	400
B10	3616	Sn117	255664
B11	4745	Sn118	271880
Na23	211380	Sb121	23261
Mg24	206270	Sb123	26674
Mg25	221188	Te125	5277
Al27	5458566	Te128	5262
Si28	1944175	Cs133	900
Si29	2455401	Ba135	41285
P31	36290	Ba137	45724
K39	211035	La139	2340
Ca43	13821852	Ce140	5543
Ca44	8750108	Ce142	7974
Sc45	803	Pr141	530
Ti47	192045	Nd146	1555
Ti49	254932	Pm147	27
V51	48417	Sm147	177
Cr52	270512	Eu153	58
Cr53	1361930	Gd157	203
Mn55	7234244	Tb159	57
Fe56	755629468	Dy163	195
Fe57	777344375	Ho165	32
Co59	54009	Er166	215
Ni60	254094	Tm169	40
Ni62	268886	Yb172	336
Cu63	316558	Lu175	24
Cu65	464592	Hf177	180
Zn66	4005079	Hf178	636
Zn67	4743591	Ta181	55
Ga69	55591	W182	99707
Ga71	55134	W183	75311
Ge72	19982	Re185	0
Ge73	17186	Os189	42
As75	37137	Ir193	0
Se77	839	Pt194	0
Se82	182	Pt195	0
Rb85	10112	Au197	0
Sr87	49161	Hg201	250
Sr88	39710	Hg202	0
Y89	1397	Tl205	50
Zr90	15458	Pb206	574184
Zr91	18690	Pb208	811786
Nb93	92643	Bi209	0
Mo95	360342	Po210	0
Mo97	408390	Th232	744
Ru101	59	Pa231	0
Rh103	59	U238	511
Pd105	561	Np237	10
Pd106	896	Pu239	3
Ag107	1055	Am241	13
Ag109	1453	Cm245	0
Cd111	9977	Bk247	0

10/20/2012

NanoSpire, Inc.

LA-ICP-MS Transmuted Particle Data

Transmuted Particle Elemental Composition by Atomic Number & Weight (SEM-EDAX & LA-ICP-MS)

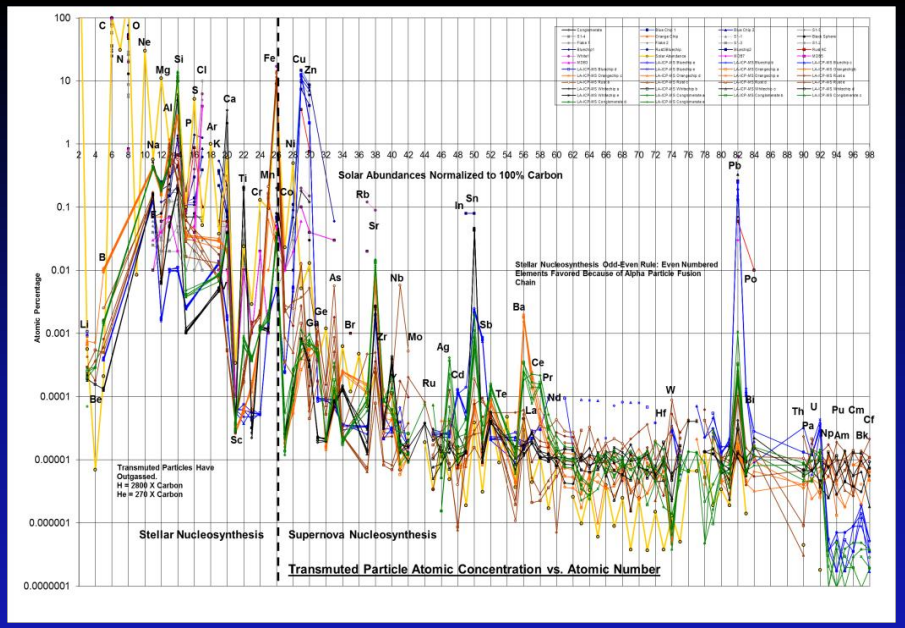

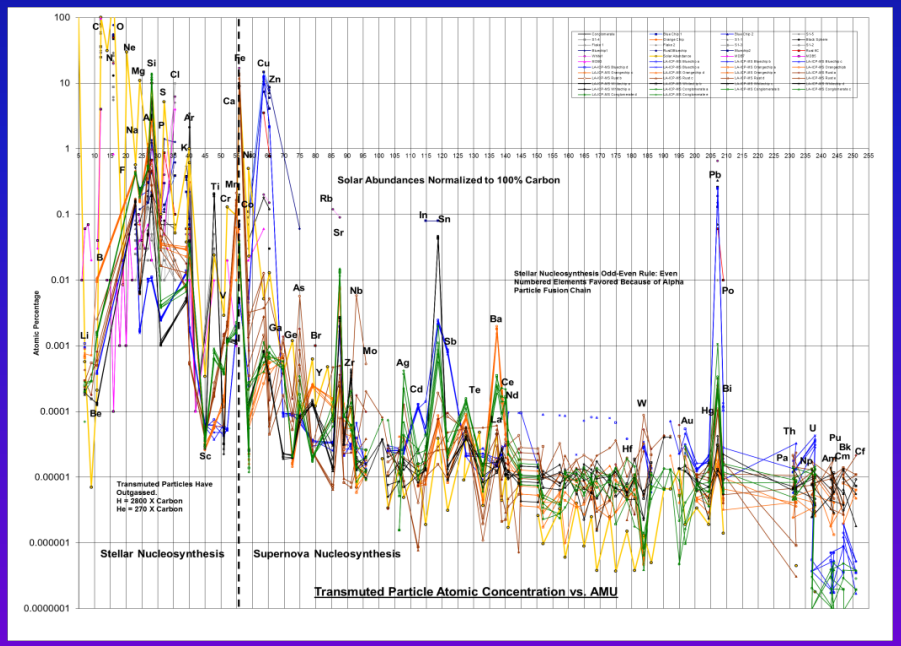

Fission Fragment Yield for Uranium & Selected Transuranic Isotopes

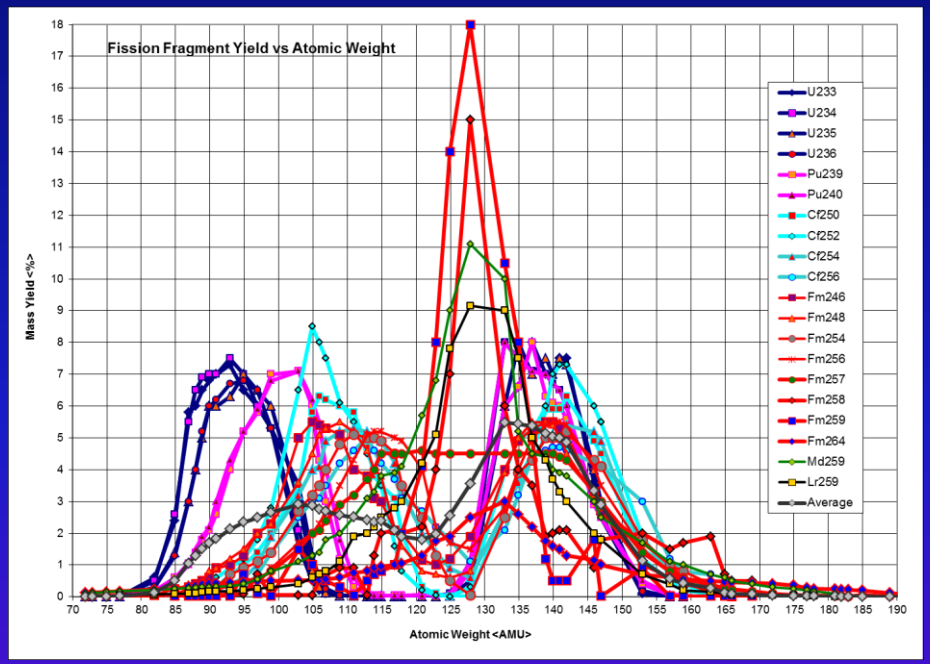

Transmuted Material Isotope Ratios vs Natural Solar Abundances

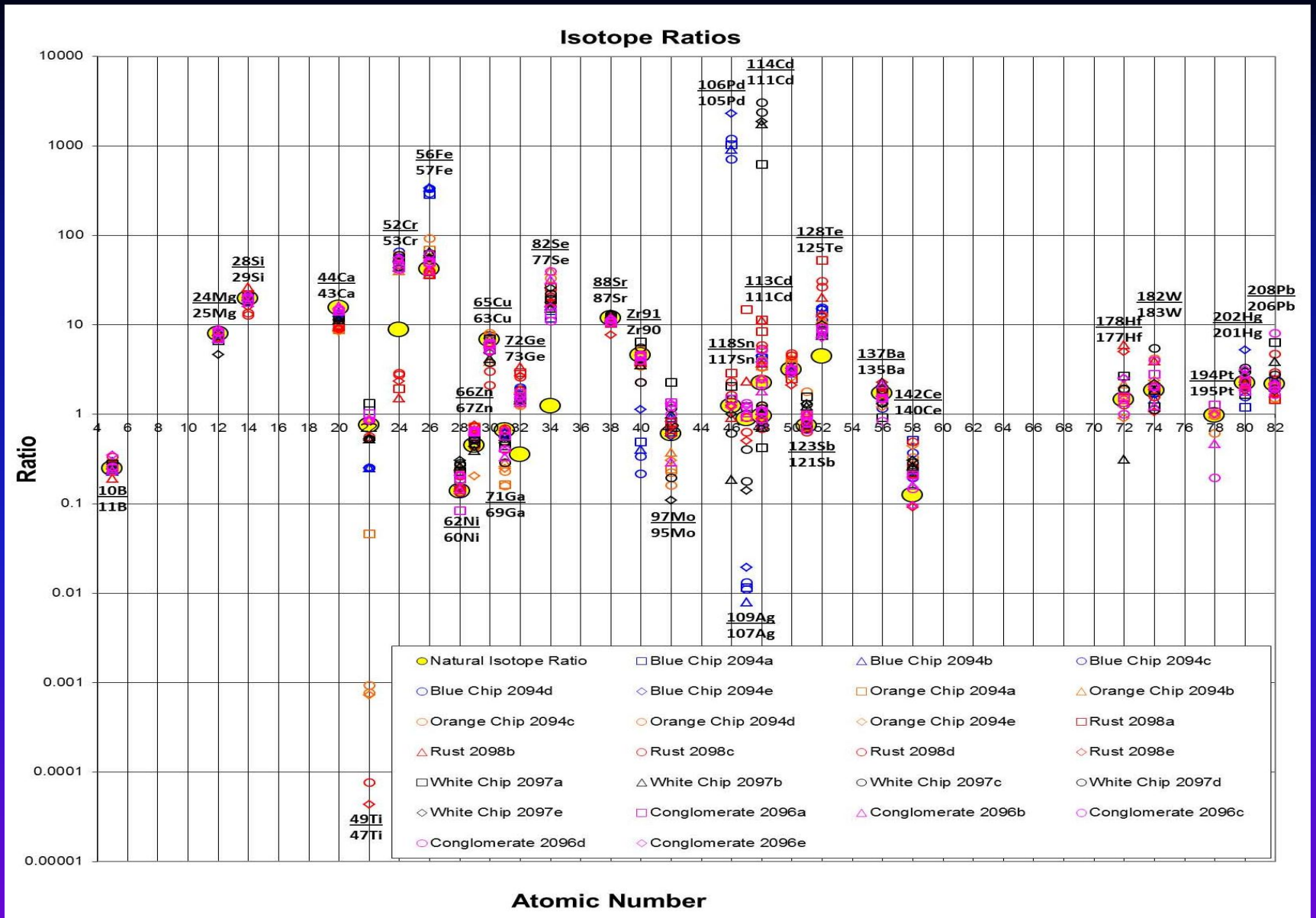

Transmuted Particle Elemental Concentration vs Carbon Concentration Similar to Supernovas

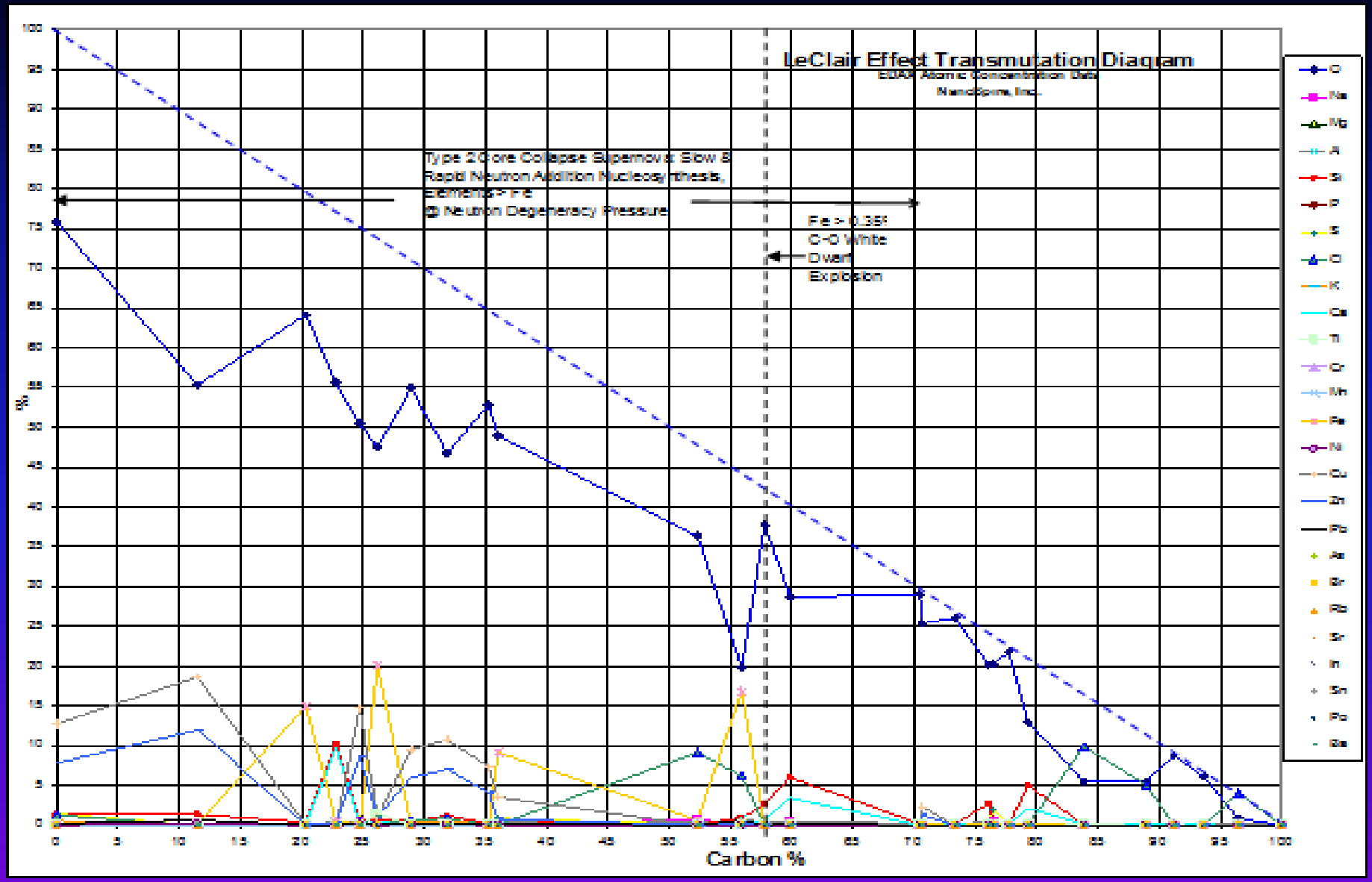

SKY (Spectral Karyotyping) Radiation Dosimetry (McMaster University)

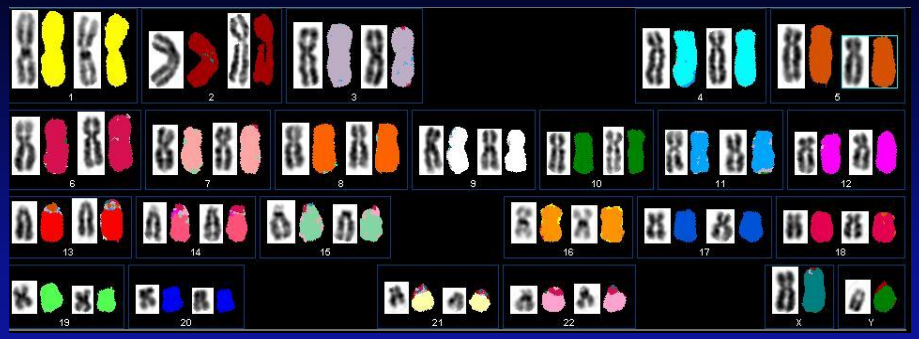

There were 3 cells that were abnormal and had chromosome aberrations. Figure 6 shows that one cell had a deletion in chromosome 2. Figure 7 shows that one cell had a translocation between chromosomes 5 and 13. Figure 8 shows that one cell contained aberrations that involved three different chromosomes involving chromosomes 2, 3 and 11.

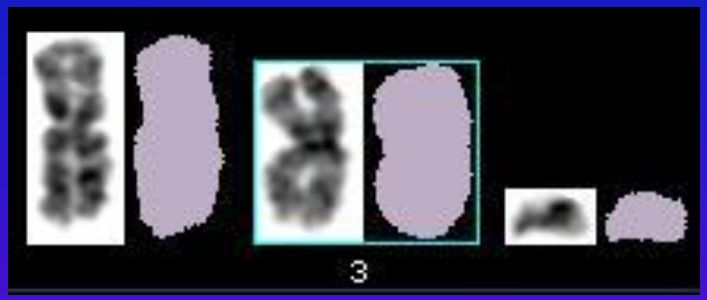

Figure 2: Chromosome 3 damage was observed in one metaphase spread. The chromosome on the left is the normal chromosome 3. The chromosome in the middle is a shorter abnormal chromosome 3 that is missing a fragment and the corresponding small fragment is seen on the right.

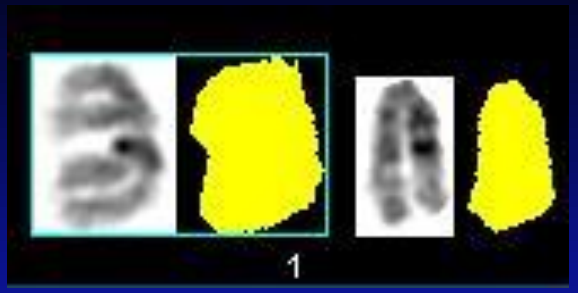

Figure 3. Chromosome 1 damage was observed in one metaphase spread. The chromosome on the left is the normal chromosome 1. The chromosome on the right is a shorter abnormal chromosome 1 that is missing a fragment. The corresponding missing small fragment was not found.

"The results from this preliminary analysis show that both donors had chromosome aberrations… It is plausible that the damage was caused by radiation. Prof. Doug Boreham"

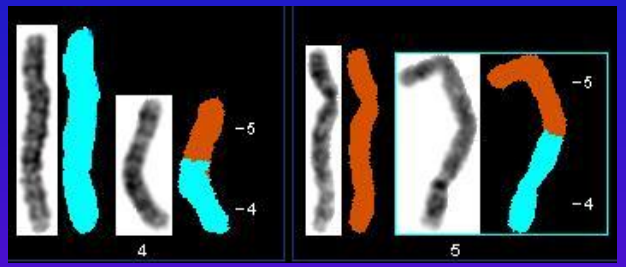

Figure 4: The left panel shows a normal chromosome 4 (blue) and an acentric fragment derived from a fusion between two fragments from chromosome 4 and 5. The left panel shows a normal chromosome 5 (red) and a dicentric chromosome derived from a fusion between two fragments from chromosomes 4 and 5.

Cavitation Fusion in Other LENR Devices

- Ultrasonics/Sonofusion:, Stringham, Impulse Devices
- Pons-Fleischmann Cells, Taleyarkhan, JET, Energetics Technologies, Ltd.
- Cavitating Rotor-Stators: Griggs Hydrosonic Pump (Hydrodynamics, Inc.), Potapov
- Brillouin? Defkalion? Rossi?

Cavitation Reentrant Jet Origin of Life Theory

Cavitation dynamics naturally create DNA, RNA and proteins, and assemble them into bacteria, archea and viruses. Primordial cavitation fusion transmutation from comet and asteroid impact into the oceans provided the bulk of elements necessary for life, not supernovas as is commonly believed

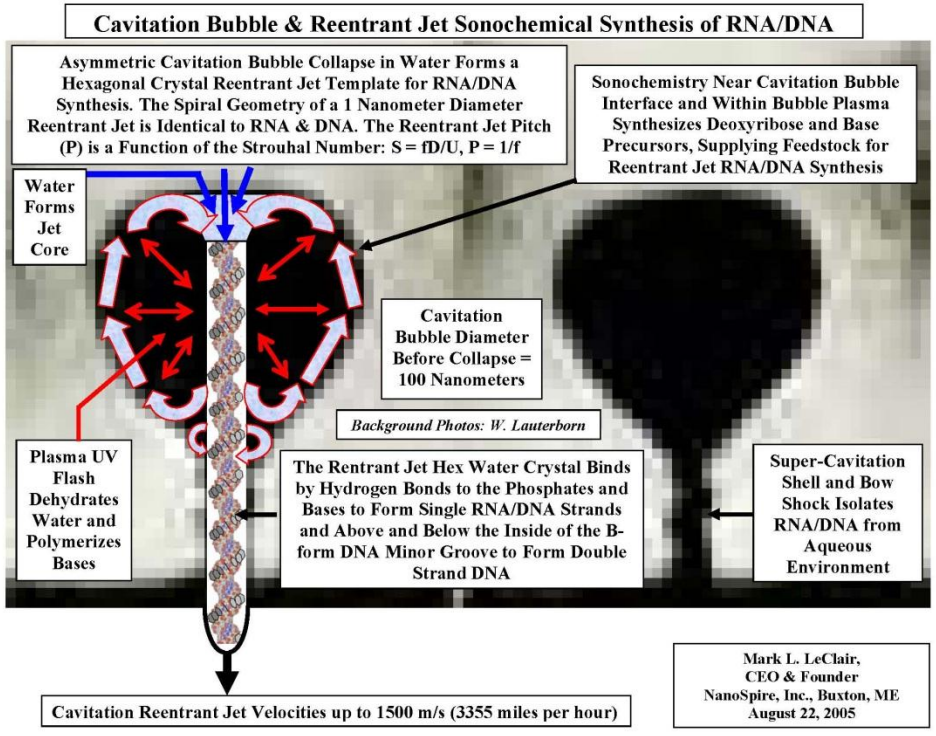

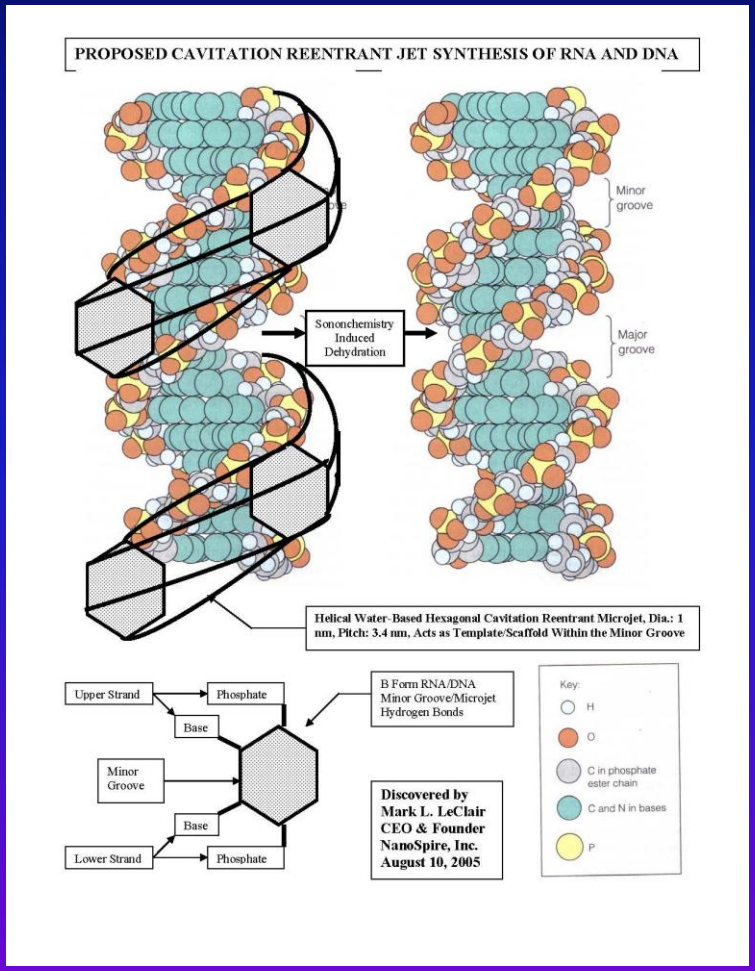

Summary

- Cavitation reentrant jets generating the LeClair Effect are the key to harnessing fusion and producing transmuted material on an industrial scale. NanoSpire's cavitation reactor generated 2900 watts of hot water flow using only 840 watts of electrical input, a coefficient of performance (COP) of 3.4

- The LeClair Effect and its theoretical predictions correctly explain excess heat and transmutation seen in many other cavitating liquid phase LENR (LeClair Effect Nuclear Reactions) devices without the need for new physics, such as heavy electrons, plasmons or other newly proposed particles or reactions. The LeClair Effect produces intense fusion with many different substrates and most importantly, even without a substrate in a liquid under the right conditions. This means that no electrochemistry, lattice-based theories, palladium, nickel, platinum, other catalysts, nanophase material or heavy water are required to produce fusion.

- Crystalized cavitation reentrant jets are the missing link, providing the ideal molecular template for synthesizing RNA, DNA & protein. Cavitation reentrant jet dynamics could have assembled the first life forms, including archea, viruses and bacteria